

University Children's Hospital of Tübingen  
Department of General Pediatrics, Haematology/Oncology

**Challenges with Gene Therapy Based on CRISPR/Cas9  
and Prime Editing for Somatic Reverted Mosaicism of  
X-linked Combined Immunodeficiency**

**Dissertation  
Submitted for a doctoral degree in Medicine**

**at the  
Faculty of Medicine  
of Eberhard-Karls-Universität  
Tübingen**

**Submitted by**

**Hou, Yujuan**

**2024**

Dean: Professor Dr. B. Pichler

First reviewer: Professor Dr. R. Handgretinger

Second reviewer: Privatdozentin Dr. C. Schneidawind

Thrid reviewer: Professor Dr. T.Cathomen

Data of oral examination: 20.02.2024.

*This thesis is dedicated to my parents Junhua & Zhihong and husband Hao  
for their support and sacrifices.*

## Contents

List of figures .....	7
List of tables .....	8
List of abbreviations .....	9
1. Introduction.....	12
X-linked severe combined immunodeficiency (X-SCID).....	12
1.1 <i>IL2RG</i> gene.....	12
1.2 Treatments.....	14
1.2.1 CRISPR/Cas9 .....	15
1.2.2. Prime editing .....	17
1.3 Aim of the study .....	18
2. Materials and Methods .....	19
2.1 Materials.....	19
2.1.1 Cells.....	19
2.1.2 Medium, supplements, growth factors and antibiotics.....	19
2.1.3 Reagents and buffers.....	20
2.1.4 Antibodies .....	20
2.1.5 Enzymes .....	20
2.1.6 Commercial kits .....	21
2.1.7 Plasmids.....	21
2.1.8 Primers and probes .....	21
2.1.9 SgRNAs and ssODNs.....	22
2.1.10 PegRNAs .....	23
2.1.11 Consumables .....	23
2.1.12 Instruments.....	24
2.2 Methods.....	25
2.2.1 Cell acquisition and culture .....	25
2.2.1.1 PBMCs isolation .....	25
2.2.1.2 CD3 <sup>+</sup> T cells .....	25
2.2.1.3 K562 cells .....	26
2.2.2 Genetic analysis.....	27

2.2.2.1 DNA extraction.....	27
2.2.2.2 DNA amplification.....	27
2.2.2.3 Amplicon visualization .....	28
2.2.2.4 DNA purification.....	28
2.2.2.5 Sanger sequencing .....	29
2.2.3 Characterization analysis .....	29
2.2.3.1 Lymphocyte percentage and IL-2R $\gamma$ expression.....	29
2.2.3.2 CD3 <sup>+</sup> T-cell proliferation .....	30
2.2.4 Gene editing by CRISPR/Cas9-ssODNs strategy.....	30
2.2.4.1 Design of sgRNAs and ssODNs .....	30
2.2.4.2 <i>In vitro</i> CRISPR/Cas9 cutting assay.....	31
2.2.4.3 SgRNAs screening in K562 and T cells.....	31
2.2.4.4 Inducing & correcting the <i>IL2RG</i> c.458T>C mutation in K562 and T cells .....	32
2.2.5 Gene editing by prime editing system .....	35
2.2.5.1 Design of pegRNAs .....	35
2.2.5.2 Plasmids mRNA <i>in vitro</i> synthesis.....	35
2.2.5.2.1 Plasmid cultivation .....	35
2.2.5.2.2 Plasmid isolation .....	36
2.2.5.2.3 Plasmid Sanger sequencing .....	36
2.2.5.2.4 Plasmid linearization.....	36
2.2.5.2.5 Plasmid visualization .....	37
2.2.5.2.6 Plasmids concentration.....	37
2.2.5.2.7 mRNA <i>in vitro</i> transcription.....	37
2.2.5.2.8 mRNA purification .....	38
2.2.5.2.9 mRNA verification .....	38
2.2.5.3 Inducing the <i>IL2RG</i> c.458T>C mutation in K562 cells.....	38
2.2.5.4 Inducing & correcting the <i>IL2RG</i> c.458T>C mutation in T cells.....	39
2.2.6 Evaluation of gene editing efficiency .....	40
2.2.6.1 DsRed and GFP expression.....	40
2.2.6.2 Sanger sequencing .....	40
2.2.6.3 Restriction fragment length polymorphism (RFLP) assay .....	40
2.2.6.4 Droplet digital PCR (ddPCR) assay .....	41

2.2.7 Statistical analysis .....	42
3. Results .....	43
3.1 Case report .....	43
3.2 Genetic analysis .....	43
3.3 Characterization analysis .....	45
3.3.1 Inverted CD4 <sup>+</sup> /CD8 <sup>+</sup> ratio .....	45
3.3.2 Normal expression of IL-2R $\gamma$ .....	45
3.3.3 Impacted proliferation of CD3 <sup>+</sup> T cells .....	46
3.4 Gene editing by CRISPR/Cas9-ssODN approach .....	47
3.4.1 sgRNAs screening for targeting <i>IL2RG</i> locus .....	47
3.4.2 Inducing the <i>IL2RG</i> c.458T>C mutation in K562 and T cells .....	51
3.4.3 Correcting the <i>IL2RG</i> c.458T>C mutation in mosaic T cells of patients .....	53
3.5 Gene editing by prime editing strategy .....	55
3.5.1 mRNA transcription of PE2 and PE2-GFP plasmids .....	55
3.5.2 Inducing the <i>IL2RG</i> c.458T>C mutation in K562 and T cells .....	55
3.5.3 Correcting the <i>IL2RG</i> c.458T>C mutation in mosaic T cells .....	59
4. Discussion .....	61
4.1 Revertant and/or hypomorphic mutation resulting in atypical X-SCID .....	61
4.2 Gene editing for nucleotide substitution of <i>IL2RG</i> in K562 and T cells .....	64
4.3 The importance of identification of genetic mosaicisms .....	66
4.4 Limitations of the study .....	67
4.5 Conclusion .....	68
5.1 Summary .....	69
5.2 Zusammenfassung .....	71
6. Bibliography .....	73
7. Declaration of Contributions to the Dissertation .....	80
8. Publications .....	81
9. Acknowledgments .....	82

## List of figures

Figure 1. Scheme of CRISPR/Cas9 system.....	16
Figure 2. Scheme of prime editing system.....	18
Figure 3. The expected fragments of RFLP assay.....	40
Figure 4. Sanger sequence of CD3 <sup>+</sup> T cells.....	44
Figure 5. Lymphocytes percentage in PBMCs.....	45
Figure 6. IL-2R $\gamma$ expression.....	46
Figure 7. Comparison of proliferation of CD3 <sup>+</sup> T-cell between patients and healthy donors.....	47
Figure 8. Scheme of <i>IL2RG</i> gene.....	48
Figure 9. <i>In vitro</i> CRISPR/Cas9 cutting assay.....	49
Figure 10. Screening sgRNAs in K562 and CD3 <sup>+</sup> T cells of healthy donors and patients.....	51
Figure 11. CRISPR/Cas9-ssODN strategy for inducing mutation (c.458C>T) in K562 and healthy donors' T cells.....	52
Figure 12. CRISPR/Cas9-ssODN transfection in mosaic T cells of patients to correct the <i>IL2RG</i> c.458T>C mutation.....	54
Figure 13. Gel visualization of linearized plasmids and synthesized mRNA <i>in vitro</i> .....	55
Figure 14. Scheme of pegRNA1.....	56
Figure 15. DsRed and GFP expression in K562 and healthy donors's T cells with prime editing strategy.....	56
Figure 16. Prime editing in K562 to induce the <i>IL2RG</i> c.458T>C mutation.....	57
Figure 17. Prime editing in T cells of healthy donors to induce the <i>IL2RG</i> c.458T>C mutation.....	58
Figure 18. Scheme of pegRNA2.....	59
Figure 19. Prime editing in mosaic T cells of patients to correct the <i>IL2RG</i> c.458T>C mutation.....	60
Figure 20. The structure of Isoleucine and Threonine.....	63

## List of tables

Table 1 List of cells employed in this work.....	19
Table 2 List of used medium, supplements, growth factors and antibiotics.....	19
Table 3 List of used reagents and buffers.....	20
Table 4 List of used antibodies.....	20
Table 5 List of used enzymes.....	20
Table 6 List of used commercial kits.....	21
Table 7 List of used plasmids.....	21
Table 8.1 List of used primers for polymerase chain reaction (PCR).....	21
Table 8.2 List of used primers and probes for droplet digital PCR (ddPCR).....	21
Table 8.3 List of used primers for inspecting the sequences of plasmids.....	22
Table 9.1 List of used sgRNAs.....	22
Table 9.2 List of used ssODNs.....	22
Table 10 List of used pegRNAs.....	23
Table 11 List of used consumables.....	23
Table 12 List of used instruments.....	24
Table 13 Preparation of PCR reaction.....	28
Table 14 PCR cycling parameters.....	28
Table 15 Components of electroporation reactions for CRISPR/Cas9-ssODNs strategy.....	33
Table 16 Culture conditions of post-transfected cells.....	34
Table 17 Ingredients of agar plates.....	35
Table 18 Ingredients of Luria Broth (LB).....	35
Table 19 Reaction for plasmids linearization.....	37
Table 20 Components of electroporation reactions for prime editing system....	39
Table 21 ddPCR cycling parameters.....	41

## List of abbreviations

AAV	Adeno-associated virus
allo-HSCT	Allogenic hematopoietic stem cell transplantation
ARCA	Anti-Reverse Cap Analog
Asn	Asparagine
auto-HSCT	Autologous hematopoietic stem cell transplantation
cDNA	Complementary DNA
CRISPR/Cas	Clustered regularly interspaced short palindromic repeat/Cas-associated proteins
<i>CYBB</i>	Cytochrome B-245 Beta Chain gene
ddPCR	Droplet Digital PCR
DPBS	Dulbecco's Phosphate Buffered Saline
DSBs	Double-strand breaks
dsDNA	Double-stranded DNA
FBS	Fetal Bovine Serum
GvHD	Graft-Versus-Host disease
<i>HBB</i>	Hemoglobin Subunit Beta gene
HDR	Homology-directed repair
HLA	Human Leukocyte Antigen
hPSCs	Human pluripotent stem cells
HR	Homologous recombination
HSCs	Hematopoietic stem cells
HSPCs	Hematopoietic stem/progenitor cells
IDT	Integrated DNA Technologies
IgG	Immunoglobulin G
IL-15	Interleukin-15
IL-2	Interleukin-2
IL-21	Interleukin-21
IL-2R	Interleukin-2 receptor
<i>IL2RG</i>	Interleukin-2 receptor gamma gene
IL-2R $\alpha$	Interleukin-2 receptor $\alpha$ chain

IL-2R $\beta$	Interleukin-2 receptor $\beta$ chain
IL-2R $\gamma$	Interleukin-2 receptor common gamma chain
IL-4	Interleukin-4
IL-7	Interleukin-7
IL-9	Interleukin-9
Ile	Isoleucine
InDels	Insertions or/and Deletions
INF- $\alpha$	Interferon-alpha
LB	Luria broth
MACS	Magnetic-activated cell sorting
nCas9	Cas9 nickase enzyme
NGS	Next Generation Sequencing
NHEJ	Nonhomologous end-joining
NK	Nature Killer cells
P/S	Penicillin/Streptomycin
P1	Patient 1
P2	Patient 2
P3	Patient 3
PAM	Protospacer adjacent motif
PBMCs	Peripheral blood mononuclear cells
PBS	Primer binding site
PCR	Polymerase chain reaction
PE	Prime editor
PE2	Prime editor 2
pegRNA	Prime-editing extended guide RNA
q-PCR	Quantitative PCR
RFLP	Restriction Fragment Length Polymorphism
RNP	Ribonucleoprotein complex
<i>RPP30</i>	Ribonuclease P/MRP Subunit P30 gene
sgRNA	Single-guide RNA
SIN-LVs	Self-inactivating lentiviral vectors
SIN- $\gamma$ RVs	Self-inactivating $\gamma$ -retroviral vectors

<i>SNCA</i>	Synuclein Alpha gene
SNV	Single nucleotide variant
ssDNA	Single-stranded DNA
ssODNs	Single-stranded DNA oligonucleotides
STAT	Signal transducer and activator of transcription signaling pathway
TALENs	Transcription activator-like effector nucleases
T-ALL	T-cell acute lymphoblastic leukemia
TH2	T helper 2 cells
Thr	Threonine
<i>TRAC</i>	T Cell Receptor Alpha Constant
Treg	Regulatory T cells
T <sub>SCM</sub>	Long-persisting memory T-cells
X-SCID	X-linked severe combined immunodeficiency
ZFNs	Zinc-finger nucleases
γRVs	γ-retroviral vectors

## 1. Introduction

### **X-linked severe combined immunodeficiency (X-SCID)**

X-linked severe combined immunodeficiency (X-SCID) is a rare primary immunodeficiency disorder caused by the interleukin-2 receptor gamma (*IL2RG*) gene mutation with X-chromosome-linked recessive inheritance. Typical X-SCID manifests as a deficiency of T and nature killer (NK) cells, and loss-functional B cells, which leads to severe and recurrent infections from bacterial, viral and fungal pathogens among others (Puck et al., 1993). Most infants with X-SCID are in a high risk of death within one year without any treatment (Gaspar et al., 2013).

#### **1.1 *IL2RG* gene**

In 1993, Noguchi et al. (Noguchi et al., 1993) firstly reported that X-SCID was caused by mutant *IL2RG* gene. Till now, more than 200 mutations have been identified in *IL2RG*. The most common type of mutation is a missense or nonsense mutation resulting from a single base change, followed by insertion or deletion mutations (Lim et al., 2019).

The *IL2RG* gene is located at X chromosome and it comprises eight exons encoding the interleukin-2 receptor common gamma chain (IL-2R $\gamma$ , also known as  $\gamma$ c). The IL-2R $\gamma$  is the shared receptor of various cytokines such as interleukin (IL)-2, 4, 7, 9, 15 and 21 (Rochman et al., 2009). Among them, IL-2, as the T-cell growth factor, is involved in T-cell proliferation and apoptosis (Sakaguchi et al., 2008). It can promote immunoglobulin production of B cells and enhances the cytotoxic effects of NK cells (Kim et al., 2006). IL-4 is required for the development and function of T helper 2 (TH2) cells, and plays an important role in immunoglobulin class switching and allergy (Holgate and Polosa, 2008). IL-7 is a lymphocyte growth factor that promotes the development of B cells derived from human bone marrow hematopoietic stem cells (HSCs) *in vitro* (Rochman et al., 2009, Parrish et al., 2009). IL-9 is

produced by activated CD4<sup>+</sup> T cells, and works in the late stage of the immune response as the T cell growth factor although the mechanism is not known (Veldhoen et al., 2008). IL-15 is essential for the development of NK cells and the homeostasis of CD8<sup>+</sup> T cells (Surh and Sprent, 2008). IL-21 drives the expansion of the CD8<sup>+</sup> T cells cooperating with IL-7 or IL-15 and is critical for apoptosis of NK cells and incompletely activated B cells (Spolski and Leonard, 2008). Furthermore, these cytokines could activate different signal transducers and activators of transcription (STAT) signaling pathway, for instance, STAT5 is activated by IL-2, IL-7, IL-9 and IL-15; STAT6 is activated by IL-4; and STAT3 is activated by IL-21 (Leonard and Spolski, 2005). Moreover, the IL-2R $\gamma$  forms the IL-2 receptor (IL-2R) with  $\alpha$  (IL-2R $\alpha$ ) and  $\beta$  (IL-2R $\beta$ ) chains together (Wang et al., 2009). To sum up, the integrity of the IL-2R $\gamma$  plays a critical role in lymphocyte development and immune function. In addition, the IL-2R $\gamma$  not only maintains the structure of the IL-2R complex, but also serves the connection between the cytokine-binding region on the surface of the cell membrane and downstream intracellular signaling molecules. Thus, the mutant *IL2RG* gene leads to defects of the IL-2R $\gamma$  in cytokine signaling that can cause immunodeficiency of typical X-SCID (Noguchi et al., 1993).

However, various mutations in the *IL2RG* gene can lead to different phenotypes of X-SCID cases. Some hypomorphic mutations, reducing but not eliminating the gene's functionality, may allow partial expression and function of IL-2R $\gamma$ . As a result, some patients showing milder clinical manifestations are not as sensitive to infections as typical X-SCID patients and present a relatively moderate decrease of T cells, normal or slightly impaired lymphocyte proliferation and STAT signaling (Brooks et al., 1990, Mella et al., 2000, Felgentreff et al., 2011). Due to these atypical phenotypes, some leaky infants of X-SCID cannot be classified by the newborn screening approaches (King and Hammarström, 2018).

Furthermore, a few X-SCID cases with revertant mutations in the *IL2RG* gene have been reported and these patients present milder clinical phenotype due to the revertant mutation presenting in one or several lymphoid populations

(Stephan et al., 1996, Kawai et al., 2012, Hsu et al., 2015, Kuijpers et al., 2013, Kury et al., 2020, Okuno et al., 2015, Speckmann et al., 2008, Lin et al., 2020, Hou et al., 2021). The revertant mutations refer to the mutant gene reversing back to wild-type sequence resulting in reversion mosaicism, which could partially or fully restore the gene functionality so it is termed as “natural therapy” (Revy et al., 2019, Aluri and Cooper, 2021). Revertant mutations could occur in different subsets of cells and the revertant cells show advantages in survival and proliferation (Kuijpers et al., 2013) that provide beneficial evidence of gene therapy for X-SCID.

## **1.2 Treatments**

Currently, the clinical treatments for X-SCID include symptomatic cures, alternative therapies, allogenic (allo-) and autologous (auto-) hematopoietic stem cell transplantation (HSCT) (Lankester et al., 2021, Haddad and Hoenig, 2019, Gaspar et al., 2013). Symptomatic treatment (e.g. prophylactic isolation, anti-infection, and nutritional support) and alternative therapies (e.g. intravenous immunoglobulin) provide only temporary relief and do not significantly improve the long-term survival and prognosis of patients (Bustamante Ogando et al., 2019, Dorsey et al., 2017), while the curative approaches of allo-HSCT and auto-HSCT could achieve immune reconstitution.

Gene therapy for X-SCID has achieved tremendous advancements since the first successful auto-HSCT in an infant with X-SCID was reported by Gatti et al. (Gatti et al., 1968) in 1968. Subsequent clinical trials of X-SCID gained promising therapeutic benefits with auto-HSCT based on gene therapy using retroviral vectors, such as gamma-retroviral and lentiviral vectors, expressing wild-type IL-2R $\gamma$ . However, some of the patients who were treated by these methods developed T-cell lymphoblastic leukemia (T-ALL) due to cellular oncogenes led by the promoter of vector integration (Hiramoto et al., 2018, Hacein-Bey-Abina et al., 2003, Hacein-Bey-Abina et al., 2008). Despite recent trials have reported that X-SCID patients treated with gene therapy using second generation of self-inactivating (SIN) vectors have obtained encouraging

clinical benefits of immune reconstitution without developing leukemia (Mamcarz et al., 2019, De Ravin et al., 2016), it needs a longer term assess the risk of insertional mutagenesis of SIN vectors (Miyazawa and Wada, 2021). To improve the feasibility and safety of gene therapy for X-SCID patients, more advance approaches of gene editing have been studied, such as zinc-finger nucleases (ZFNs) (Schiroli et al., 2017), transcription activator-like effector nucleases (TALENs) (Menon et al., 2015), RNA-guided nucleases (CRISPR/Cas) (Pavel-Dinu et al., 2019) and nuclease-free (adeno-associated viruses (AAV) (Hiramoto et al., 2018). These methods have shown very promising results in *in vitro* and *in vivo* pre-clinical studies of several genetic diseases.

### **1.2.1 CRISPR/Cas9**

The CRISPR/Cas system is engineered from the antiviral bacterial immune system. It consists of single-guide RNA (sgRNA) and Cas9 endonuclease. In brief, DNA double helix is unraveled after Cas9 recognizes the appropriate protospacer adjacent motif (PAM), and sgRNA binds the target sequence to complex an RNA-DNA heteroduplex. At this point, the conformation of Cas9 is changed due to the formation of the R-loop, which activates the cutting function of Cas9 and cleaves the DNA strands, generating the double-strand breaks (DSBs). There are two main pathways to repair the induced DSBs: nonhomologous end-joining (NHEJ) and homologous recombination (HR) (Hartlerode and Scully, 2009). NHEJ repair is fallible as it could generate unexpected insertions and/or deletions (indels) at the DSBs site (Symington and Gautier, 2011), which leads to it being restricted to the knockout and disruption of genes. NHEJ repair is susceptible to occur throughout the whole cell cycle, while homology-directed repair (HDR) pathway only happens in the S and G2 phases, which limits HDR efficiency in the process of DNA repair (Liu et al., 2018). Since HDR has high fidelity, it is generally used to specific genomic edits such as substitutions, desired insertions or deletions with a suitable donor template for effective DNA repair (Her and Bunting, 2018). The templates are usually delivered as three main forms: plasmid or double-stranded DNA

(dsDNA), adeno-associated virus (AAV), and single-stranded DNA (ssDNA). The donor template is usually co-delivered to the cells with the CRISPR/Cas9 component, either as ribonucleoprotein (RNP) complex, mRNA or DNA plasmid (Devkota, 2018).

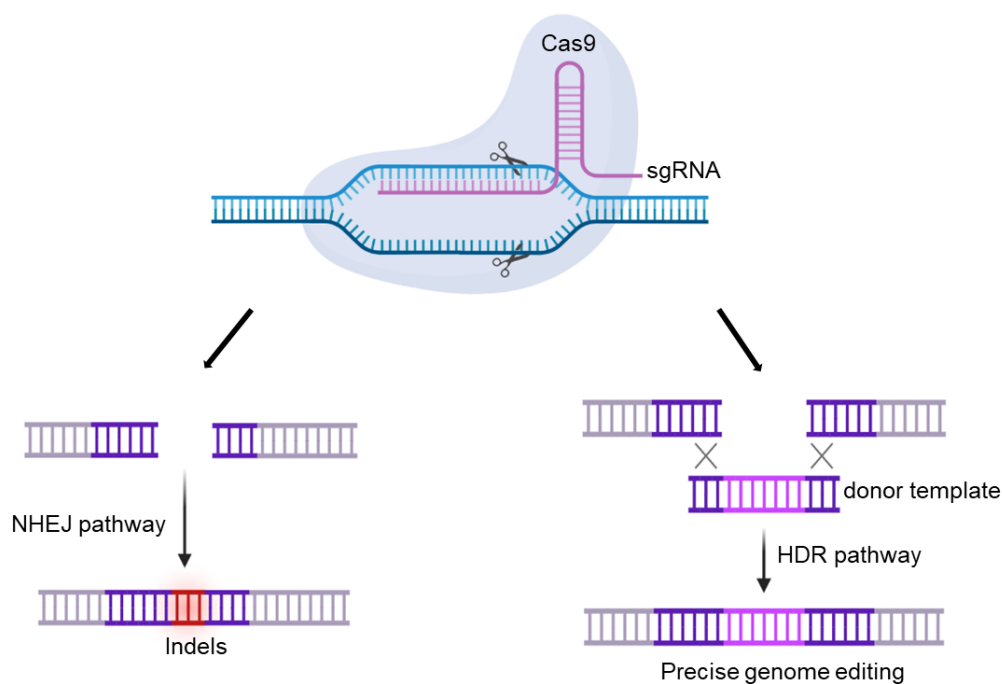


**Figure 1.** Scheme of CRISPR/Cas9 system. The sgRNA binds the Cas9 and targets the specific genome locus, then the Cas9 cuts DNA strands after recognizing the protospacer adjacent motif (PAM sequence). The double-strand breaks (DSBs) of DNA can be repaired either non-homologous end joining (NHEJ) resulting in insertions or deletions of random nucleotides, or homologous directed repair (HDR) with a suitable donor template leading to specific gene correction. (The image was created with BioRender.com)

Although ssDNA oligonucleotides (ssODNs) are limited to inserting short sequences and their optimized design is unclear so far, it is one of the most employed strategies as the design is easier than other methods and its synthetic production is faster and cheaper (Romero et al., 2019). In the previous studies using CRISPR/Cas9 strategy and ssODNs to correct the single nucleotide mutations, DeWitt *et al.* (DeWitt et al., 2016) reported 33% of HDR frequency targeting Hemoglobin Subunit Beta (*HBB*) gene mutation (c.20 A>T) in hematopoietic stem/progenitor cells (HSPCs). Wen *et al.* (Wen et al., 2017)

corrected the *HBB* gene (c.20 A>T) and achieved 9% HDR efficiency in HSPCs. De Ravin *et al.* (De Ravin *et al.*, 2017) edited the Cytochrome B-245 Beta Chain (*CYBB*) gene (C676T) in HSPCs with 21% HDR rate. Compared to other formats such as AAV or dsDNA, ssODN reduces the off-target frequency and toxicity (Romero *et al.*, 2019).

### **1.2.2. Prime editing**

Because CRISPR/Cas9 mediated DSBs presents low HDR efficiencies, safety concerns due to genomic instability, and PAM restriction, more advanced genome editing tools have been emerged. Prime editing is a more precise "search-and-replace" gene editing technique that can carry out small deletions, insertions and base-base substitutions without the requirements of DSBs or exogenous donor DNA templates (Anzalone *et al.*, 2019). The system includes a prime-editing RNA that is made up of a sgRNA, a primer binding site (PBS), and a template that contains the desired sequence which is referred to as a reverse transcript template or RT template. Another component of the system is the prime editor (PE), which combines Cas9 nickase (nCas9) and reverse transcriptase (Anzalone *et al.*, 2019). The concise mechanism is: after PE-pegRNA complex binds to the target sequence, nCas9 cleaves the PAM-containing DNA strand, and the 3' flap of the target strand complements the pegRNA to initiate reverse transcription; then the unmodified 5' flap is excised and the broken end is joined by DNA ligase to generate the heteroduplex constituting with one edited strand and one unedited strand; subsequently, with the completion of new DNA duplex carrying the target modification under the DNA genetics mechanism, precision editing is achieved (Anzalone *et al.*, 2019). Compared to CRISPR/Cas9 system, prime editing offers higher efficiency and less off-target (Li *et al.*, 2022).

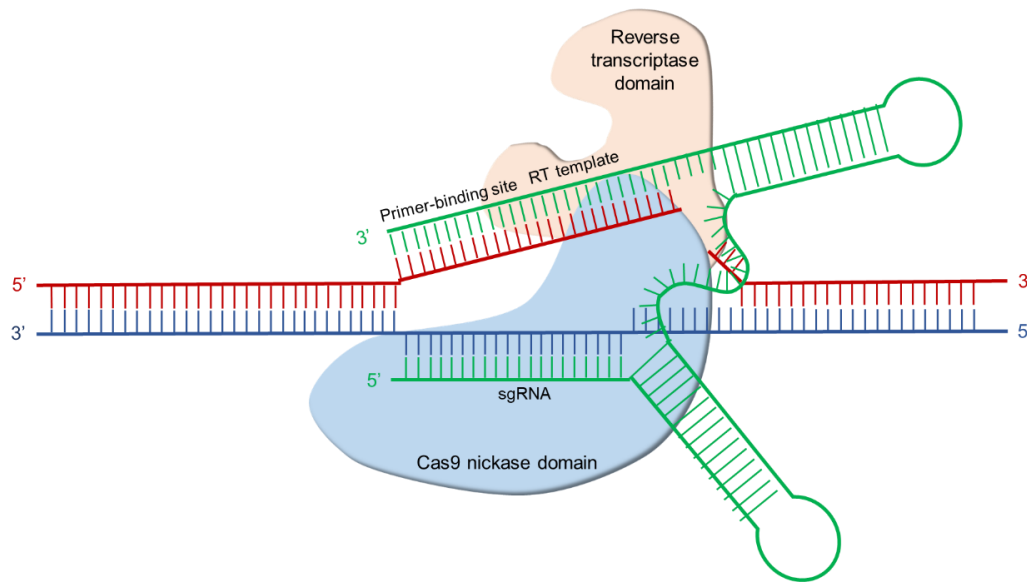


**Figure 2.** Scheme of prime editing system. Prime editing is a more accurate genome editing technique that directly complete the genomic edit at the specified DNA site using a catalytically impaired Cas9 fused to an engineered reverse transcriptase (RT), programmed with a prime editing guide RNA (pegRNA) specifying the target site and encoding the desired modification. (The image was created with BioRender.com and PowerPoint)

### 1.3 Aim of the study

Due to the novel mutation c.458T>C (p.Ile153Thr) in *IL2RG* and rare somatic mosaicism exhibited, this project aims to characterize this new mutation with partial reversion, as well as discuss the possibilities of gene therapy targeting the mutant *IL2RG* (c.458T>C) gene for X-SCID patients in mosaic T cells using CRISPR/Cas9-ssODN and prime editing approaches.

## 2. Materials and Methods

### 2.1 Materials

#### 2.1.1 Cells

**Table 1** List of cells employed in this work.

Cell Type	Source/Supplier	Culture
PBMC	Healthy donors & patients	-
CD3 <sup>+</sup> T cell	Healthy donors & patients	TexMACS medium, + 1% Penicillin/Streptomycin (P/S), + 10 ng/mL IL-7 & 5 ng/mL IL-15 (for healthy donors) or 50 units/ml IL-2 (for patients).  Incubation at 37 °C with 5% CO <sub>2</sub> .
K562 cell line	Sigma-Aldrich	RPMI1640 medium, + 10% Fetal Bovine Serum (FBS), +1% L-glutamine, + 1% P/S.  Incubation at 37 °C with 5% CO <sub>2</sub> .

#### 2.1.2 Medium, supplements, growth factors and antibiotics

**Table 2** List of used medium, supplements, growth factors and antibiotics.

Item	Manufacturer
TexMACS medium	Miltenyi Biotec
RPMI 1640 medium	Biochrom GmbH
Fetal Bovine Serum (FBS), heat inactivated	ThermoFisher Scientific
L-glutamine	Sigma-Aldrich
Interleukin-2	Miltenyi Biotec
Interleukin-7	Miltenyi Biotec
Interleukin-15	Miltenyi Biotec
Penicillin	ThermoFisher Scientific
Streptomycin	ThermoFisher Scientific
Ampicillin	Carl Roth GmbH
TransAct™	Miltenyi Biotec

### 2.1.3 Reagents and buffers

**Table 3** List of used reagents and buffers.

Item	Manufacturer
Biocoll separation solution	Biochrom GmbH
CD3 <sup>+</sup> MicroBeads	Miltenyi Biotec
ddPCR oil	Bio-Rad
ddPCR SuperMix for probes (no dUTP)	Bio-Rad
Electrolytic buffer E	Invitrogen
Electrolytic buffer R	Invitrogen
Electrolytic buffer T	Invitrogen
Ethanol	ThermoFisher Scientific
Gel loading dye purple 6X	New England Biolabs
GelRed	Biotium
Lithium chloride	ThermoFisher Scientific
MACS buffer	Miltenyi Biotec
Nuclease-free water	ThermoFisher Scientific
Dulbecco's Phosphate Buffered Saline	Sigma-Aldrich
Quick-load purple 100bp DNA ladder	New England Biolabs
Quick-load purple 1kb DNA ladder	New England Biolabs
SeaKem <sup>®</sup> LE Agarose	Lonza
ssRNA ladder	New England Biolabs
TAE buffer 10X, pH 8.5	ThermoFisher Scientific
TE Buffer	Synthego
Trypan blue	ThermoFisher Scientific
Ultra-Pure Agarose	Invitrogen

### 2.1.4 Antibodies

**Table 4** List of used antibodies.

Antibody	Species	Manufacturer
Anti-CD3	human	Miltenyi Biotec
Anti-CD4	human	Miltenyi Biotec
Anti-CD8	human	Miltenyi Biotec
Anti-CD14	human	Miltenyi Biotec
Anti-CD19	human	Miltenyi Biotec
Anti-CD56	human	Miltenyi Biotec

### 2.1.5 Enzymes

**Table 5** List of used enzymes.

Enzyme	Manufacturer
Alt-R <sup>®</sup> S.p. Cas9 Nuclease V3	Integrated DNA Technologies (IDT)
GoTaq Green DNA polymerase	Promega
Proteinase K	Macherey Nagel
<i>PmeI</i>	NEW England Biolabs
<i>MseI</i>	NEW England Biolabs
<i>DpnII</i>	NEW England Biolabs

## 2.1.6 Commercial kits

**Table 6** List of used commercial kits.

Kit	Manufacturer
Ambion® Anti-Reverse Cap Analog (ARCA)	ThermoFisher Scientific
MEGAscript T7 transcription kit	ThermoFisher Scientific
NucleoSpin Tissue	Macherey Nagel
Poly(A) Tailing	Ambion
QIAGEN Plasmid Maxi	QIAGEN
QIAquick PCR purification	QIAGEN

## 2.1.7 Plasmids

**Table 7** List of used plasmids.

Plasmid	Vector backbone	Gene/Insert name	Manufacturer
pCMV-PE2	pCMV	PE2	Addgene (#132775)
pCMV-PE2-P2A-GFP	pCMV	PE2-P2A-GFP	Addgene (#132776)
pCS2 <sup>+</sup> DsRed	pCS2 <sup>+</sup>	DsRed	Gift from Prof. Michael Kormann

\* The plasmid of pCMV-PE2 is termed PE2 and pCMV-PE2-P2A-GFP is PE2-GFP in the text.

## 2.1.8 Primers and probes

**Table 8.1** List of used primers for polymerase chain reaction (PCR).

Gene	Item	Sequence (5'→3')	Amplicon length	Source
<i>IL2RG</i>	Forward	AGGCCACACAGATGCTAAAAC	409 bp	Own design
	Reverse	TGCTACATTCACGTCCCTAGT		
<i>TRAC</i>	Forward	ATCACGAGCAGCTGGTTTCT	636 bp	(Osborn et al., 2016)
	Reverse	CCCGTGTCATTCTCTGGACT		

**Table 8.2** List of used primers and probes for droplet digital PCR (ddPCR).

Gene	Item	Sequence (5'→3')	Source
<i>IL2RG</i>	Forward primer	TATTAGGGGCACTACCTTC	BIO-RAD
	Reverse primer	TTGTGAAGTGTTAGGTTCTC	
	Edited Probe	CCAGGGGATCACTGGA	
	Native Dark Probe	CCAGGGGGTCACTGGA	
<i>RPP30</i>	Forward primer	AGATTTGGACCTGCCGAGCG	(Profaizer and Slev, 2020)
	Reverse primer	GAGCGGCTGTCTCCACAAGT	
	Probe	TTCTGACCTGAAGGCTCTGCGCG	

\*Edited probe of *IL2RG* gene targets wild-type sequence while native dark probe binds mutant sequence.

**Table 8.3** List of used primers for inspecting the sequences of plasmids.

Item	Sequence (5'→3')
Primer 1	AATGTCGTAACAACCTCCGCC
Primer 2	TGGAAGAGTCCTTCTGGTG
Primer 3	CAGTACGCCGACCTGTTTCTG
Primer 4	TCGAGGAAGTGGTGGACAAGG
Primer 5	AGCAGTCCGGCAAGACAATC
Primer 6	TGACCAGAAGCGACAAGAACC
Primer 7	TTCAAGACCGAGATTACCCTGG
Primer 8	CTCCCCCGAGGATAATGAGC
Primer 9	AGGGTCCACATGGCTGTCTG
Primer 10	TGAGGCACTGCACAGAGACC
Primer 11	GCCTATCAAGAAATCAAGCA
Primer 12	TGCGGTGACCACCGAGACCG
Primer 13	AGCCATCACAGAGACTCCAG
Primer eGFP	CCAGGATGTTGCCGTCCTCC

\*Primers1-13 were used for plasmids of PE2 and PE2-GFP; primer eGFP was only for PE2-GFP.

## 2.1.9 SgRNAs and ssODNs

**Table 9.1** List of used sgRNAs.

Gene	Sequence (5'→3')	Target Sequence	Source
<i>IL2RG</i>	sgRNA1	ACATATCTCCAGTGATCCCTGG	Wild-type
	sgRNA2	TTAGGTTCTCTGGAGCCCAGGG	Wild-type & Mutant
	sgRNA3	TAGGTTCTCTGGAGCCCAGGG	Mutant
	sgRNA4	TCTGGAGCCCAGGGG <u>G</u> TCACTGG	Mutant
	sgRNA5	TCTGGAGCCCAGGGGATCACTGG	Wild-type
	sgRNA6	GGTGCAGTACCGGACTGACTGG	Wild-type & Mutant
<i>TRAC</i>	GAGAATCAAATCGGTGAATAAA	-	(Osborn et al., 2016)

\* Underline base in sgRNAs of *IL2RG* correspond to mutation; last three nucleotides marked in red is PAM.

**Table 9.2** List of used ssODNs.

	Sequence (5'→3')	Aim	Size
ssODN 1	A*T*C*CTGACTTGTCTAGGCCAGGGGAATGACCACAT ATGCACACATATCTCCAGTGA <u>C</u> CCCCTGGGCTCCAGA GAACCTAACACTTCACAACTGAGTGAATCCCAGCTA GAACTGAACTGGAA*C*A*A	inducing mutation	126 nt
ssODN 2	C*C*A*GGGGAATGACCACATATGCACACATATCTCCA GTGA <u>C</u> ACCCTGGGCTCCAGAGAACCTAACACTTCACA AACT*G*A*G	inducing mutation	79 nt
ssODN 3	A*G*G*AGGTATTAGGGGCACTACCTTCAGGATCCTGA CTTGTCTAGGCCAGGGGAATGACCACATATGCACACA TATCTCCAGTGA <u>T</u> CCCCTGGGCTCCAGAGAACCTAAC ACTTCACAACTGAG*T*G*A	correcting mutation	127 nt
ssODN 4	A*T*C*CTGACTTGTCTAGGCCAGGGGAATGACCACAT ATGCACACATATCTCCAGTGA <u>T</u> CCCCTGGGCTCCAGA GAACCTAACACTTCACAACTGAGTGAATCCCAGCTA GAACTGAACTGGAA*C*A*A	correcting mutation	126 nt

\* The marked nucleotides in green aim to correct the mutation and the red ones aim to induce mutation.

## 2.1.10 PegRNAs

**Table 10** List of used pegRNAs.

	<b>Sequence (5'→3')</b>	<b>Aim</b>	<b>Size</b>
pegRNA 1	U*U*A*GGUUCUCUGGAGCCCAGGUUUUAGAGCUAG AAAUAGCAAGUUAAAAUAAGGCUAGUCCGUUAUC AACUUGAAAAAGUGGCACCGAGUCGGUGCAGUG A <b>C</b> CCCCUGGGCUCCAGAG*A*A*C	inducing mutation	121 nt
pegRNA 2	UAGGUUCUCUGGAGCCCAGGGUUUUAGAGCUAG AAAUAGCAAGUUAAAAUAAGGCUAGUCCGUUAUC AACUUGAAAAAGUGGCACCGAGUCGGUGCUCCA GUGA <b>U</b> CCCCUGGGCUCCAG*A*G*A	correcting mutation	122 nt

\* The marked nucleotides in green aim to correct the mutation and the red ones aim to induce mutation.

## 2.1.11 Consumables

**Table 11** List of used consumables.

<b>Item</b>	<b>Volume</b>	<b>Manufacturer</b>
Cell culture plates	24, 48, 96 wells	Corning Costar
ddPCR plate	96 wells	Bio-Rad
DG8 Cartridges	-	Bio-Rad
Droplet generator DG8 Gasket	-	Bio-Rad
Falcon tubes	15mL, 50mL	Greiner Bio-One
Filter tips	10µL, 100uL, 200µl, 1,000µL	TipOne
Microcentrifugation tubes	500uL, 1.5mL, 2mL	Eppendorf
PCR tubes	200uL	ThermoFisher Scientific
Pipette tips	10µl, 100uL,200µL, 1,000µL	Corning Costar
Pipette tips	5mL,10mL, 25mL, 50mL	Corning Costar

## 2.1.12 Instruments.

**Table 12** List of used instruments.

<b>Instrument</b>	<b>Manufacturer</b>
Biological Safety Cabinet	Thermo Fisher Scientific
Centrifuge Mikro22R	Hettich
Centrifuge Rotina420R	Hettich
Erlenmeyer flasks (100mL, 250mL)	Thermo Fisher Scientific
BD FACS Calibur flow cytometer	BD Biosciences
Fridge 4°C	Liebherr
Freezer -20°C	Bosch
Freezer -80°C	Forma Scientific
HeraCell Incubator	Thermo Fisher Scientific
Improved Neubauer cell chamber (hemacytometer)	Marienfield
Light microscope	Zeiss
MiniGel2 electrophoresis system	VWR
MiniSpin centrifuge	Heathrow Scientific
Nanodrop 2000	Thermo Fisher Scientific
Neon <sup>®</sup> electroporator	Invitrogen
Neon <sup>®</sup> 10µl pipette	Invitrogen
Pipettes (10µL, 20µL, 100µL, 200µL, 1000µL)	Brand
Thermalcycler C1000 Touch	BioRad
Thermoblock	Thermo Fisher Scientific
Vortex reax 2000	Heidolph
GTX Transfection	MaxCyte

## **2.2 Methods**

The study was performed in accordance with the Institutional Review Board approval from the University of Tübingen Ethics Committee (No. 928/2020BO2).

### **2.2.1 Cell acquisition and culture**

The peripheral blood mononuclear cells (PBMCs) and CD3<sup>+</sup> T cells from peripheral blood were isolated from patients and age-matched healthy donors after informed consent. PBMCs were studied to clarify the percentage of lymphocytes and IL-2R $\gamma$  expression in different subtypes of lymphocytes. CD3<sup>+</sup> T cells were used to induce and correct the mutation in *IL2RG* gene by CRISPR/Cas9 and prime editing systems. K562 cell line was employed to establish the transfection protocol and detect the potential efficacy of gene-editing since K562 cell line is easily cultured and the transfection protocol using Neon Electroporation system has been previously established in our lab (Lamsfus-Calle et al., 2021).

#### **2.2.1.1 PBMCs isolation**

PBMCs were harvested by traditional Ficoll density gradient centrifugation. Briefly, blood and PBS were mixed 1:1 in volume, the mixture was added slowly to the equal volume of Biocoll<sup>®</sup> and centrifugated at 20°C, 1/R1, 800g, 30 min. PBMCs' white ring was taken slowly by the pipette in a rotating manner and washed with PBS twice (total volume up to 50mL). The pellet of PBMCs was collected after centrifugations: 20°C, 9/R9, 500g, 10min (1st washing); 20°C, 9/R9, 400g, 10min (2nd washing). Then 10 $\mu$ L of resuspended cells were mixed with Trypan Blue at specific dilutions and counted in a Neubauer chamber under a light microscope.

#### **2.2.1.2 CD3<sup>+</sup> T cells**

CD3<sup>+</sup> T cells were isolated with Magnetic-activated cell sorting (MACS) system (CliniMACS System, Miltenyi Biotec) according to the protocol from the manufacturer. Following the above steps of PBMCs isolation, the cells were

washed for one more time and were pelleted at 4°C, 9/R7, 200g, 10min. Afterwards, up to 10<sup>7</sup> of PBMCs were resuspended in 80µL of pre-shaken, cold MACS buffer, as well as labeled by 20µL of CD3<sup>+</sup> MACS<sup>®</sup> MicroBeads. After 15 minutes incubation at 4°C, the cells were washed again with MACS buffer (1.5ml each 10<sup>7</sup> of cells) and gathered after centrifugation (4°C, 9/R9, 300g, 10min). The pellet was resuspended in MACS buffer (500µL for up to 10<sup>8</sup> cells), then applied to the LS column placed at the magnetic field of the MACS Separator and soaked by 3mL of MACS buffer in advance. Magnetically labeled CD3<sup>+</sup> T cells were retained within the column, while CD3<sup>-</sup> cells flowed through. After triple washing with 3mL of MACS buffer, the LS column was removed from the magnetic separator. The target cells were eluted with 5ml of MACS buffer by applying pressure with the syringe. CD3<sup>+</sup> T cells were isolated by positive selection with CD3<sup>+</sup> MACS MicroBeads. After washing 3 times with RPMI 1640 medium at 4°C, CD3<sup>+</sup> T cells were counted with light microscope.

The purification of CD3<sup>+</sup> T cells was corroborated in flow cytometry analyses. Cells were stained with human CD3, CD4, CD8, CD45 (positive T-cell markers) and CD14, CD19 (negative T-cell markers) antibodies and incubated for 10 min at room temperature in the dark. Then, the stained cells were washed with PBS and suspended in 100µL of PBS. In the end, the cells were acquired on FACS Calibur flow cytometer (BD Biosciences) and analyzed with FlowJo software (the purity of CD3<sup>+</sup> T cells was more than 90% for all experiments).

Subsequently, every one million of cells were expanded by 10 µL of TransAct and cultured in 1mL of TexMACS medium supplemented with 1% P/S, 10 ng/mL IL-7 and 5 ng/mL IL-15 for healthy donors or 50 units/mL IL-2 for patients, at 37 °C with 5% CO<sub>2</sub>.

### **2.2.1.3 K562 cells**

K562 cells were used to establish the gene-editing protocols of this study. The cell line was originally derived from Sigma-Aldrich. Frozen K562 cells were recovered and thawed quickly in 37°C water bath. When only a little ice was left in the cryovial, the cell solution (1mL) was transferred into 20mL of fresh RPMI1640 medium with 10-20% FBS to neutralize the toxicity of the DMSO,

and centrifuged at 400g for 5 min, following two washings with RPMI1640 medium. Afterwards, K562 cells were cultured in RPMI1640 medium supplemented with 10% FBS, 1% L-glutamine, and 1% P/S at 37 °C with 5% CO<sub>2</sub>.

### **2.2.2 Genetic analysis**

To confirm the mutation (c.458T>C) in the *IL2RG* gene, genetic analyses were performed by Sanger sequencing.

#### **2.2.2.1 DNA extraction**

The genomic DNA was isolated from cells using NucleoSpin Tissue kit following the user manual. Firstly, cells pellets were acquired in 1.5mL microcentrifuge tube by centrifugation (20°C, 9/R9, 400g, 5min). Up to 10<sup>7</sup> cells were resuspended in 200µL Buffer T1, subsequently 25µL Proteinase K solution and 200µL Buffer B3 were added before incubation at 70 °C for 15 min to lysate the cells. After adding 210µL ethanol (100 %) to the lysate to improve DNA binding to the silica membrane in the NucleoSpin® Tissue Columns, the mixture was applied to the column with the collection tube and centrifuged. The column carrying genomic DNA was placed back into the collection tube and washed twice with 500µl Buffer BW and 600µl Buffer B5 by centrifugation. Another centrifugation was done to dry silica membrane and remove residual ethanol. Pure genomic DNA was eluted with 30µL of pre-warmed nucleotide-free water into the 1.5mL tube and centrifuged after incubating for 1 min at room temperature. All centrifugation settings during DNA isolation were performed for 1 min with 11,000xg at room temperature.

Finally, the DNA concentration was measured using NanoDrop 2000 by loading 1µL of pre-mixed samples. All genomic DNA samples were stored at -20°C.

#### **2.2.2.2 DNA amplification**

The genomic region covering the *IL2RG* mutation (409bp) was amplified in a PCR reaction using the following pair of primers: forward: AGGCCACACAGATGCTAAAAC; reverse: TGCTACATTCACGTCCCTAGT.

The *TRAC* region (636 bp) was amplified with forward primer: ATCACGAGCAGCTGGTTTCT and reverse primer: CCCGTGTCATTCTCTGGA CT. The reaction preparation and PCR settings are shown in the tables below:

**Table 13** Preparation of PCR reaction mixes on ice.

		Volume (uL)	Final concentration
Genomic DNA		X	5ng/μL
Primers	Forward (5μM)	1	250nM
	Reverse (5μM)	1	250nM
GoTaq® Green Master Mix		10	2X
Nucleotide-free water		8-X	-
Total		20	

**Table 14** PCR cycling parameters.

Step	Temperatura	Time	Cycles number
Initial Denaturation	95°C	2 min	1
Denaturation	95°C	40 s	40
Annealing	62°C ( <i>IL2RG</i> ) & 55°C ( <i>TRAC</i> )	30 s	
Extension	68°C	1 min	
Hold	4°C	∞	-

### 2.2.2.3 Amplicon visualization

Amplicon of PCR products were visualized by the Odyssey FC Imaging System (LI-COR) after separation by electrophoresis on 1% agarose gel at 100 Volts for 30 min. For this purpose, 1g of agarose was dissolved in 100mL 1x TAE buffer and boiled in a microwave at 600 W for 1 min. 5μL of GelRed® was mixed into the liquid after cooling for 2 min. Then, the solution was added to the prepared chamber for electrophoresis and gelified after incubation at room temperature for 30 min. 5μL of 100bp DNA ladder and 6μL of products were applied to the gel, respectively. Eventually, Odyssey FC Imaging System was used to develop the membrane.

### 2.2.2.4 DNA purification

PCR products were purified by QIAquick PCR purification kit (Qiagen). 5 volumes of PB buffer were added and mixed to each volume of PCR production. The mixes were transferred to QIAquick columns in 2mL collection tubes and

centrifuged, then washed with 750 $\mu$ L PE buffer. After centrifuging to remove residual wash buffer, purified DNA amplicon was eluted with 30 $\mu$ L of pre-warmed nucleotide-free water into the 1.5mL microcentrifugation tube and centrifuged after incubating for 1 min at room temperature. All centrifugation settings during DNA purification are 1 min at 17,900xg at room temperature.

The DNA concentration was confirmed by Nanodrop 2000.

#### **2.2.2.5 Sanger sequencing**

The samples in the volume of 17 $\mu$ L were mixed by purified DNA (75ng), 4 $\mu$ L of the forward primer (5 $\mu$ M) and Nucleotide-free water, and sent to Eurofins Genomics company for Sanger sequencing analysis. The reported data were analyzed by ApE software to compare the difference in target sequence between patients and healthy donors.

#### **2.2.3 Characterization analysis**

To clarify and study the characteristics of this novel mutation on the *IL2RG* gene, the following experiments were implemented.

##### **2.2.3.1 Lymphocyte percentage and IL-2R $\gamma$ expression**

To compare the percentage of lymphocytes and IL-2R $\gamma$  expression on subsets of lymphocytes between patients and healthy donors, the fluorescence staining was carried out using PBMCs. Isolated PBMCs were incubated with human antibodies of CD132(IL2-R $\gamma$ )-PE, CD3-FITC, CD4-PerCP, CD8-APC, CD14-APC, CD19-FITC, CD56-PerCP for 10 min at room temperature in the dark. After washing and resuspending in 100 $\mu$ L of PBS, the cells were acquired on FACS Calibur flow cytometer (BD Biosciences) and analyzed by FlowJo software. Suitable cell populations were gated for different purposes and comparison of IL-2R $\gamma$  expression was carried out between experimental and control samples.

### 2.2.3.2 CD3<sup>+</sup> T-cell proliferation

To study the proliferation of patients' CD3<sup>+</sup> T cells *ex vivo*, 2 different proliferation assays were performed. All cells isolated from patients and healthy donors were expanded by TransAct as description on section 2.2.1.2. 300,000 cells were seeded in 48-well plates, in triplicate, with 200µL of medium. 200µL fresh medium was given every 2 days.

- Stimulation with IL-7 plus IL-15: Cells were cultured in supplemented TexMACS medium (10% FBS, 1% P/S) with IL-7 and (10 ng/mL) and IL-15 (5 ng/mL).
- Stimulation with IL-2: Cells were cultured in supplemented TexMACS medium (10% FBS, 1% P/S) with IL-2 (50 units/mL).

Cell counting was carried out by flow cytometer on days 1, 3, 5, 7 and 9 with the mix of 10uL cells and 90uL PBS. Calibur flow cytometer was used to acquire all liquid to determine the number of cells in 10uL followed by FlowJo analysis to calculate the total number of cultured cells. The proliferation of T cells was presented as fold-change which is the ratio of the number of cells between the counting day (DayZ) and the first day (Day1).

$$\text{Fold-change} = \frac{(\text{The number of cells in } 10\mu\text{L} / 10\mu\text{L}) * \text{total volume on DayZ}}{\text{The number of cells on Day1}}$$

### 2.2.4 Gene editing by CRISPR/Cas9-ssODNs strategy

#### 2.2.4.1 Design of sgRNAs and ssODNs

The sgRNAs of *IL2RG* gene with 20nt length were designed by online CHOPCHOP software (<https://chopchop.cbu.uib.no/>) to target the *IL2RG* c.458T>C mutation on Exon4. All sgRNAs were synthesized by IDT (Coralville, IA, USA) with chemically 2'-O-methyl 3'phosphorothioate modification (**Table 9.1**).

The ssODNs were designed using horizon online tool (<https://horizondiscovery.com/en/ordering-and-calculation-tools/edit-r-hdr-donor-designer-oligo>) to induce (ssODN 1/2) and correct (ssODN 3/4) the mutation at

the site of c.458 *IL2RG* gene. They were synthesized by Metabion ([www.metabion.com](http://www.metabion.com)) with chemical modification of 3'phosphonothioate 2'-O-methyl in three terminal nucleotides at both 5' and 3' ends (**Table 9.2**).

#### **2.2.4.2 *In vitro* CRISPR/Cas9 cutting assay**

To evaluate the cutting potential of designed sgRNAs for *IL2RG*, *in vitro* CRISPR/Cas9 cutting assay was performed according to the *in vitro* cleavage protocol to target DNA from IDT. As previously described (Antony et al., 2022), the reaction including the 100nM of PCR product (Section **2.2.2.2**) and ribonucleoprotein (RNP) complex of 200nM sgRNA and 100nM Cas9 protein was incubated at 37°C for 2 hours and stopped by adding proteinase K (Macherey Nagel) and incubation for 10 minutes at 56°C. Agarose gel electrophoresis (1%) for 30 min at 100V was done to visualize the resulting products.

#### **2.2.4.3 SgRNAs screening in K562 and T cells**

In order to investigate the editing efficiency of CRISPR/Cas9 with designed sgRNAs, sgRNAs screening was performed using cultured K562, isolated CD3<sup>+</sup> T cells from healthy donors (3 days after activation and expansion) and CD3<sup>+</sup> T cells from patient (1 day after activation). The RNP was prepared by mixing of 90pmol of each sgRNAs (*IL2RG* or *TRAC*) and 45pmol of Cas9 V3 protein (IDT) and incubated at room temperature for 15 minutes. Moreover, 1µg DsRed mRNA was also transfected as the electroporation positive control. 100,000 cells were transfected using Neon electroporator and 10µL Neon transfection kit (Thermo Fisher Scientific) with the following electroporation settings: 1450V, 10ms, 3 pulses for K562 cells, and 1800V, 10ms, 3 pulses for T cells. Following transfection, the cells were transferred to the 48-well plate with 400µL pre-warmed supplemented RPMI-1640 medium for K562 (Section **2.2.1.3**) and TexMACS medium for T cells (Section **2.2.1.2**). 200µL of fresh medium was added to cells every 2 days.

Furthermore, cell proliferation assay was performed for CD3<sup>+</sup> T cells from healthy donors using flow cytometry (BD FACS Calibur) on day 1, 3 and 5 post-electroporation with RNP (Section **2.2.3.2**).

#### **2.2.4.4 Inducing & correcting the *IL2RG* c.458T>C mutation in K562 and T cells**

To induce or correct the *IL2RG* mutation, GTX Transfection System with R-50X3 electroporation assemblies (50µL volumen in each electroporation reaction, MaxCyte) was used to delivery RNP complex (sgRNA and Cas9 at molar ratio of 2:1) and ssODN to K562 cells, T cells of healthy donors (activated and expanded for 3 days post isolation) and patients (activated and expanded for one day post isolation).

The cells were harvested and counted by microscope using Trypan Blue (Thermo Fisher Scientific) staining to check for the viability (>80%), then were pelleted by centrifugation for 5 minutes at 400g after washing with PBS and resuspended in HyClone electroporation buffer (MaxCyte) at a density of 5x10<sup>7</sup> cell/mL (for K562 cells) or 3x10<sup>7</sup> cell/mL (for T cells) as cell mastermix.

RNPs were incubated for 15 min at room temperatura, then placed on ice before using. The 50µL cell mastermix were added to the RNP complex, then the ssODN was added to the reaction right before electroporation. The final mixes were transferred to the cuvettes and electroporations were carried out with selected programs.

DsRed mRNA was transfected (5µg mRNA into 50µL reaction) as electroporation control in every independent experiment.

The amount of components (sgRNAs, Cas9 protein, ssODNs) and the concentration of cells are detailed in the **Table 15**. The selected electroporation protocols of GTX system are “K562” for K562 cells and “Expanded T cell 3” for T cells. After electroporation, the transfected cells were seeded in the plates (warm-up and in the incubator in advance to get moisture) and recovered at 37°C for 30 min, then cultured in corresponding medium at 37 °C with 5% CO<sub>2</sub>. The culture conditions of post-transfected cells are showed in **Table 16**.

**Table 15** Components of electroporation reactions for CRISPR/Cas9-ssODNs strategy.

Cells	Sample	Component	Amount	Final concentration (μM)	Loading agent (μL)	Number of cells for each reaction
K562 cells (inducing mutation)	DsRed control	DsRed mRNA	5μg	-	-	2.5x10 <sup>6</sup>
	ssODN control	ssODN 1/2	300pmol	6.00	3.00	
		KO control	sgRNA2	150pmol	3.00	
	KI		Cas9 protein	75pmol	1.50	
		KI	sgRNA2	150pmol	3.00	
	KI		Cas9 protein	75pmol	1.50	
T cells of healthy donors (inducing mutation)		DsRed control	DsRed mRNA	5μg	-	-
	ssODN control	ssODN 1/2	300pmol	6.00	3.00	
		KO control	sgRNA2	200pmol	4.00	2.00
	KI		Cas9 protein	100pmol	2.00	1.64
		KI	sgRNA2	200pmol	4.00	2.00
	KI		Cas9 protein	100pmol	2.00	1.64
T cells of patients (correcting mutation)		DsRed control	DsRed mRNA	5μg	-	-
	ssODN control	ssODN 3/4	300pmol	6.00	3.00	
		KO control	sgRNA 3/4	200pmol	4.00	2.00
	KI		Cas9 protein	100pmol	2.00	1.64
		KI	sgRNA 3/4	200pmol	4.00	2.00
	KI		Cas9 protein	100pmol	2.00	1.64
KI		ssODN 3/4	300pmol	6.00	3.00	

\* KO: knock-out; KI: knock-in, the modified samples; Stock concentrations of sgRNAs and ssODNs were 100μM, Cas9 protein was 61μM.

**Table 16** Culture conditions of post-transfected cells.

Cells	Sample	Seeding density (cell/mL)	Volume culture needed (mL)	Culture plate	Culture medium
K562 cell line (inducing mutation)	DsRed control	1x10 <sup>6</sup>	2.50	6-well	<ol style="list-style-type: none"> <li>100µL cell mastermix (50µL electroporation mastermix and 50µL washed buffer) to recover for 30 min;</li> <li>2400uL RPMI1640 medium supplied with 10% FBS, 1% L-glutamine, 1% P/S was added.</li> </ol>
	ssODN control				
	KO control				
	KI				
T cells of healthy donors (inducing mutation)	DsRed control	1x10 <sup>6</sup>	1.50	24-well	<ol style="list-style-type: none"> <li>100uL cell mastermix (50µL electroporation mastermix and 50µL washed buffer) to recover for 30 min;</li> <li>650µL TexMACS medium without supplements was added;</li> <li>After 4 hours, 750µL TexMACS medium supplied with 20 ng/mL IL-7 &amp; 10 ng/mL IL-15 was added.</li> </ol>
	ssODN control				
	KO control				
	KI				
T cells of patients (correcting mutation)	DsRed control	1x10 <sup>6</sup>	1.50	24-well	<ol style="list-style-type: none"> <li>100uL cell mastermix (50µL electroporation mastermix and 50µL washed buffer) to recover for 30 min;</li> <li>650µL TexMACS medium without supplements was added;</li> <li>After 4 hours, 750µL TexMACS medium supplied with 100 units/mL IL-2 was added.</li> </ol>
	ssODN control				
	KO control				
	KI				

\* KO: knock-out; KI: knock-in, the modified samples.

## 2.2.5 Gene editing by prime editing system

### 2.2.5.1 Design of pegRNAs

The pegRNAs were designed by pegFinder online tool (<http://pegfinder.sidichenlab.org/>) and were synthesized by IDT with Phosphonothioate 2'-O-methyl modification (**Table 10**).

### 2.2.5.2 Plasmids mRNA *in vitro* synthesis

Plasmids of pCMV-PE2 (PE2) and pCMV-PE2-P2A-GFP (PE2-GFP) (Anzalone et al., 2019) were purchased from Addgene (pCMV-PE2 #132775; pCMV-PE2-P2A-GFP #132776. <https://www.addgene.org>).

#### 2.2.5.2.1 Plasmid cultivation

Plasmids were provided in bacteria stocks by the manufacturer. To proceed with plasmid maxipreparations, bacteria were inoculated in agar plates (**Table 17**) including ampicillin. Single colonies were isolated by streaking the plates and were incubated at 37°C for 14-16 hours. Then, single colonies were picked up under the flame of a Bunsen burner and transferred to Erlenmeyer flasks with 150mL of Luria broth (LB) culture medium containing ampicillin (ingredients of LB medium in **Table 18**). The culture was incubated at 37 °C overnight with shaking at 800 rpm.

**Table 17** Ingredients of agar plates.

Ingredient	Volume
Milipore Water	1,000 mL
Agar	15 g
Luria Broth (LB)	25 g
Ampicillin	100 mg

**Table 18** Ingredients of Luria Broth (LB).

Ingredient	Volume
Milipore Water	1,000 mL
Luria Broth (LB)	25 g
Ampicillin	100 mg

#### **2.2.5.2.2 Plasmid isolation**

Plasmids were isolated using the QIAGEN Plasmid Maxi Kit (QIAGEN) following the manufacturer's instructions. The cultured bacterial carrying plasmids were harvested by centrifugation at  $6000 \times g$  for 15 min at  $4 \text{ }^{\circ}\text{C}$  and then resuspended in 10mL Buffer P1, as well as 10mL Buffer P2 by mixing thoroughly by vigorously inverting 4-6 times. The mixtures were incubated at room temperature for 5 min. After that, 10mL pre-chilled Buffer P3 was added to the mixture by vigorously inverting 4-6 times to mix well and incubate on ice for 20 min. One centrifugation for the mixture was performed at  $\geq 20,000 \times g$  for 30 min at  $4 \text{ }^{\circ}\text{C}$ , and another one for supernatant coming from the former at  $\geq 20,000 \times g$  for 15 min at  $4 \text{ }^{\circ}\text{C}$ . During the time of centrifugation, a QIAGEN-tip 500 was equilibrated by applying 10mL Buffer QBT and allowed the column to empty by gravity flow. Next, the supernatant after centrifuging was applied to the QIAGEN-tip and allowed to enter the resin by gravity flow. Afterwards, the QIAGEN-tip was washed twice with 30mL Buffer QC which was allowed to move through the QIAGEN-tip by gravity flow. DNA was proceeded to elute with 15mL Buffer QF into a clean 50mL vessel and mixed with 10.5mL room-temperature isopropanol. The mixture was centrifuged at  $\geq 15,000 \times g$  for 30 min at  $4 \text{ }^{\circ}\text{C}$ . After decanting the supernatant, the DNA pellet was washed with 50mL room-temperature 70% ethanol and centrifuged again with the former setting. At last, the pellet was dissolved in 250 $\mu\text{L}$  of TE Buffer post air-dry. Concentration of DNA was measured by NanoDrop 2000.

#### **2.2.5.2.3 Plasmid Sanger sequencing**

Sanger Sequencing of plasmids was carried out by Eurofins Genomics company. The samples were sent after preparing 15 $\mu\text{L}$  of plasmid DNA (100ng/ $\mu\text{L}$ ) and 15 $\mu\text{L}$  of corresponding primers (5 $\mu\text{M}$ ). A total of 14 primers were used to assess the full sequence of the plasmids (**Table 8.3**). Sequencing results verified the sequence of PE2 and PE2-GFP (results not shown).

#### **2.2.5.2.4 Plasmid linearization**

The reactions were prepared on the ice as indicated below and then incubated at  $37 \text{ }^{\circ}\text{C}$  for 2 hours.

**Table 19** Reaction for plasmids linearization.

Reagent	Volume ( $\mu\text{L}$ )	Final concentration
Plasmid	X	200ng/ $\mu\text{L}$
<i>pMel</i>	5	1units/ $\mu\text{L}$
rCutSmart buffer	5	10X
Nuclease-free water	40-X	-
	50	

\* X was calculated by the stock concentration of plasmids. The amount of plasmid was 10 $\mu\text{g}$  for every 50 $\mu\text{L}$  of reaction.

#### **2.2.5.2.5 Plasmid visualization**

Plasmid visualization was performed by electrophoresis on 1% agarose gel at 100V for 30 min and carried out the result with Odyssey FC Imaging System. 5 $\mu\text{L}$  of 1Kb DNA ladder was applied to the gel. 0.5 $\mu\text{L}$  of non-linearized plasmids (as the control) and 0.5 $\mu\text{L}$  of linearized plasmids were separately mixed with 4.5 $\mu\text{L}$  of Nuclease-free water and 1 $\mu\text{L}$  of DNA Gel Loading Dye (6X).

#### **2.2.5.2.6 Plasmids concentration**

The remaining 49.5 $\mu\text{L}$  of linearized plasmids were purified by mixing 2.5 $\mu\text{L}$  (1:20) of EDTA (0.5M), 4.95 $\mu\text{L}$  (1:10) of NH<sub>4</sub> acetate (5M) and 24.75 $\mu\text{L}$  (1:2) of ethanol (100%) and chilled at -20 °C for 15 min. A subsequent centrifugation step was carried out at top speed for 15 min to precipitate the DNA, which was eventually resuspended in 10 $\mu\text{L}$  of TE buffer.

DNA concentration was determined by NanoDrop 2000. Plasmid was stored at -20°C.

#### **2.2.5.2.7 mRNA *in vitro* transcription**

The mRNA *in vitro* transcription was performed with linearized plasmids using the MEGAscript T7 transcription kit. 20 $\mu\text{L}$  reaction was mixed with 1 $\mu\text{g}$  of the plasmid (dissolved in 5 $\mu\text{L}$  Nuclease-free water), 2 $\mu\text{L}$  10X Reaction buffer, 2 $\mu\text{L}$  GTP (diluted in Nuclease-free water to 1:5) & ATP & CTP & UTP, 2 $\mu\text{L}$  T7 polymerase, 3 $\mu\text{L}$  Ambion® Anti-Reverse Cap Analog (ARCA, ThermoFisher Scientific) and incubated at 37°C for 2 hours. Then, 1 $\mu\text{L}$  TURBO™ DNase (Thermo Fisher Scientific) was added at 37° C for 15 min to degrade the DNA template from the reaction. The following reagents were loaded: 20 $\mu\text{L}$  5X E-PAP buffer, 10 $\mu\text{L}$  MnCl<sub>2</sub> (25nM), 10 $\mu\text{L}$  ATP (10mM), and 36 $\mu\text{L}$  Nuclease-free water. After mixing by pipetting, 0.5 $\mu\text{L}$  aliquot was took out for non-

polyadenylated control and 4µL poly A polymerase was added to the rest of the reaction, incubating at 37°C for 1 hour to polyadenilate the mRNA.

#### **2.2.5.2.8 mRNA purification**

30µL nuclease-free water and 30µL LiCl precipitation solution were added to stop the tailing reaction. Next, the mixture was incubated at -20°C for 30 min and centrifuged with maximum speed at 4°C for 15min. The pellet of mRNA was obtained after removing the supernatant. Washing with 1mL ethanol (70%) and centrifugation with maximum speed at 4°C for 15min were needed to maximize the removal of unincorporated nucleotides.

#### **2.2.5.2.9 mRNA verification**

Purified mRNA was visualized on the 1% UltraPure Agarose gel by electrophoresis. 2µL RNA ladder was mixed with 8uL Nuclease-free water and 2µL DNA Gel Loading Dye (6X). 0.5µL of non-polyadenylated control or polyadenilated samples were mixed with 9.5µL Nuclease-free water and 2µL DNA Gel Loading Dye (6X). Samples were loaded and gel electrophoreses ran for 30 min at 100V. Then the size and polyadenilation of mRNA was corroborated by the Odyssey FC Imaging System.

The concentration of the mRNAs was determined using NanoDrop 2000.

The mRNAs were stored in aliquots at -80° C.

#### **2.2.5.3 Inducing the *IL2RG* c.458T>C mutation in K562 cells**

After washing and pelleting  $3 \times 10^5$  of K562 cells, the cells were suspended in 10µL electroporation NEON Buffer R (Thermo Fisher Scientific), and then 1µg of either PE2 or PE2-GFP mRNA and 90pmol pegRNA1 were added to the cells. The transfection was performed by NEON Transfection System (Thermo Fisher Scientific) with the following parameters: 1450V, 10ms, 3 pulses. DsRed mRNA (1µg) was transfected as positive control of electroporation. The transfected cells were transferred to 48-well plate with 400µL pre-warmed supplemented RPMI1640 medium. The day after transfection, 400µL of fresh medium was added to the cells.

### 2.2.5.4 Inducing & correcting the *IL2RG* c.458T>C mutation in T cells

To induce the c.458T>C *IL2RG* mutation into healthy donors' T cells and correct this mutation in patients' T cells, transfections of PE2/PE2-GFP mRNA and pegRNA were carried out by GTX Transfection System using Cuvette R-50X3. The preparation of T cells of healthy donors and patients are detailed in Section 2.2.4.4.

For each reaction,  $1.5 \times 10^6$  cells were suspended in 50 $\mu$ L HyClone electroporation buffer (MaxCyte) and mixed with 5 $\mu$ g of PE2 or PE2-GFP mRNA, and 150pmol of pegRNA 1 (for inducing the mutation in healthy donors' T cells) or pegRNA 2 (for correcting the mutation in patients' T cells, **Table 20**). The mixtures of cells and prime editing component were loaded to the cuvette and electroporated using the "Expanded T cell 3" program. After electroporation, the cells were recovered at 37°C for 30 min on a 96-well round-bottom plate, then transferred to 24-well plate containing 650 $\mu$ L warm TexMACS media without any supplementation. After 4 hours, 750 $\mu$ L TexMACS medium supplemented with 20ng/mL IL-7 and 10ng/mL IL-15 was added to the healthy donors' T cells and 750 $\mu$ L TexMACS medium supplied with 100 units/mL IL-2 was added to the patient T cells to make  $1 \times 10^6$  cells/mL density of cells. Culture conditions of transfected T cells is detailed in **Table 16**.

**Table 20** Components of electroporation reactions for prime editing system

Cells	Sample	Component	Amount	Final concentration
T cells of healthy donors (inducing mutation)	DsRed control	DsRed mRNA	5 $\mu$ g	100ng/ $\mu$ L
	PE2	pegRNA 1	150pmol	3 $\mu$ M
		PE2 mRNA	5 $\mu$ g	100ng/ $\mu$ L
	PE2-GFP	pegRNA 1	150pmol	3 $\mu$ M
PE2-GFP mRNA		5 $\mu$ g	100ng/ $\mu$ L	
T cells of patients (correcting mutation)	DsRed control	DsRed mRNA	5 $\mu$ g	100ng/ $\mu$ L
	PE2	pegRNA 2	150pmol	3 $\mu$ M
		PE2 mRNA	5 $\mu$ g	100ng/ $\mu$ L
	PE2-GFP	pegRNA 2	150pmol	3 $\mu$ M
PE2-GFP mRNA		5 $\mu$ g	100ng/ $\mu$ L	

## 2.2.6 Evaluation of gene editing efficiency

### 2.2.6.1 DsRed and GFP expression

The day after electroporation, cells transfected by DsRed or PE2-GFP mRNA were analyzed by flow cytometry after washing with PBS once using the BD FACS Calibur. Results were subsequently analyzed by FlowJo software and DsRed or GFP expression was quantified.

### 2.2.6.2 Sanger sequencing

Genomic analysis of modified cells was performed by Sanger Sequencing. For K562 cells, gDNA was isolated on day5 after transfection, while for transfected T cells with prime editing, gDNA was acquired on day2, and the gDNA of modified T cells with CRISPR/Cas9-ssODN was obtained on day5 post electroporation. Genomic DNA isolation, PCR and Sanger sequencing were carried out as described in **Section 2.2.2**. SYNTHOGO online Inference of CRISPR Edits (ICE) tool (<https://ice.synthego.com/#/>) (ICE analysis) was used to detect the insertion and deletion (InDels) rate and gene-editing efficiency by analyzing the data from Sanger Sequencing of edited samples.

### 2.2.6.3 Restriction fragment length polymorphism (RFLP) assay

RFLP assay was performed to detect the induced mutation by prime editing on K562 cells and CD3<sup>+</sup> T cells from healthy donors. 200ng of PCR product was incubated with 5units of *DpnII* (NEB) in total volume of 10µl at 37°C for 2 hours. The digestion process was stopped by incubating of reaction at 65°C for 20 min. 5µL of digested and undigested samples was mixed with 1µL DNA Gel Loading Dye (6X) (NEB) and loaded on the 2.5% agarose gel for electrophoresis. The wild type sequence was expected to generate 167bp, 143bp, 55bp, 44bp fragments and the mutated allele was expected to generate fragments with 222bp, 143bp, 44bp length (**Figure 3**).

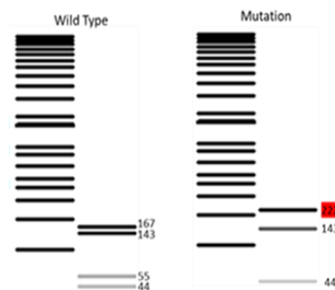


**Figure 3.** The expected fragments of RFLP assay with digestion of *DpnII* enzyme in wild-type (167bp, 143bp, 55bp, 44bp) and mutant (222bp, 143bp, 44bp) sequences respectively. (The image was created by Ape software)

#### 2.2.6.4 Droplet digital PCR (ddPCR) assay

The ddPCR assay was performed to quantify the gene-editing efficiency of prime editing approach separately. The primers and probes were designed and synthesized by Bio-Rad. The primers and probe of *RPP30* (reference gene) were obtained from a previous publication (Profaizer and Slev, 2020) and synthesized by IDT company. The sequences of probes and primers are presented in **Table 8.2**.

Firstly, 20µL of ddPCR reaction was mixed with 50ng of gDNA, 5units of restriction endonuclease *MseI* (NEB), 1X of ddPCR™ Supermix for Probes (No dUTP) (Bio-Rad), 900nM of primers and 250nM of probes of *IL2RG* and *RPP30* genes, and nuclease-free water, and was incubated at room temperature for 15 min. Then, the reactions, as well as 70µL of droplet generating oil (Bio-Rad) for each reaction, were loaded into the DG8™ Cartridges (Bio-Rad) to generate droplets using the QX200™ Droplet Generator. After that, 42µL of droplet-mixture were transferred into a 96 deep-well reaction plate (Bio-Rad), sealed with PX1 PCR Plate Sealer (Bio-Rad) and run on the thermocycler following program (**Table21**).

**Table 21** ddPCR cycling parameters.

Cycling step	Temperature °C	Time	Ramp Rate	Number of cycles
Enzyme activation	95	10 min	2 °C/ sec	1
Denaturation	94	30 sec		40
Annealing /Extension	55	1 min		1
Enzyme deactivation	98	10 min		1
Hold	4	∞		1

Subsequently, droplet readings were performed by the QX200 Droplet Reader and the data was analyzed with QuantaSoft software (version 1.7.4, Bio-Rad). The difference in the ratio of *IL2RG* (copies/ul)/*RPP30* (copies/ul) between edited samples and the control was used to calculate the editing efficiency.

### **2.2.7 Statistical analysis**

The statistical analysis was performed using the Graph Pad Prism 9.1.2 software (GraphPad Software, San Diego, CA, USA). Unpaired t-test was applied to compare lymphocyte percentage between patients and healthy donors. And Ordinary one-way ANOVA test was used to compare the proliferation rate between transfected healthy donors' T cells with *IL2RG* sgRNAs and Cas9 and non-transfected cells ( $p < 0.05$ , \*  $< 0.05$ , \*\*  $< 0.01$ , \*\*\*  $< 0.001$ , \*\*\*\*  $< 0.0001$ ).

### 3. Results

#### 3.1 Case report

Three 20-year-old brothers were born from nonconsanguineous, disease-free German parents. Patient 1 (P1) has been suffering from opportunistic respiratory and viral infections. He suffered from infectious molluscum contagiosum at the age of 6 years and skin warts on his hands and feet at the age of 11 years. Topical IL-2 injections, imiquimod cream, cryotherapy and retinoids of treatments did not improve his condition significantly. Then the subcutaneous interferon alpha (INF-) relieved some of his warts, but this therapy was interrupted due to severe side effects of recurrent fever and alopecia. In addition, chronic respiratory infections and bronchiectasis occurred after the patient had severe lung infections twice. P1 was treated with immunoglobulin and anti-microbial prophylaxis at 19 years old due to a suspected immunodeficiency. After that, no further serious bacterial or viral infections were reported, although skin warts persist. At 21 years old, a molecular genetics diagnostic study revealed the *IL2RG* c.458T>C mutation. Subsequently, it was confirmed that his mother is carrier of this mutation and two brothers (Patient 2, P2, and Patient 3, P3) share the same mutation. P2 and P3 also had suffered from respiratory infections and skin warts in the teenage period, but with lower severity and fewer episodes than P1.

#### 3.2 Genetic analysis

To confirm the presence of the *IL2RG* c.458T>C mutation, the Sanger sequencing of CD3<sup>+</sup> T cells from patients and their mother was performed. Compared to the healthy donor (**Figure 4.A**), patients' mother is the heterozygote carrying the *IL2RG* c.458T>C mutation (**Figure 4.B**). Noteworthy, in patients' cells, the coexistence of the mutant (c.458C) and wild-type (c.458T) nucleotides was observed (**Figure 4.C**). Furthermore, the genetic analysis of proliferated CD3<sup>+</sup> T cells of P1 showed that the frequency of the mutant

sequence was reduced with culture time *in vitro* (64% on day1 to 47% on day5) (Figure 4.D).

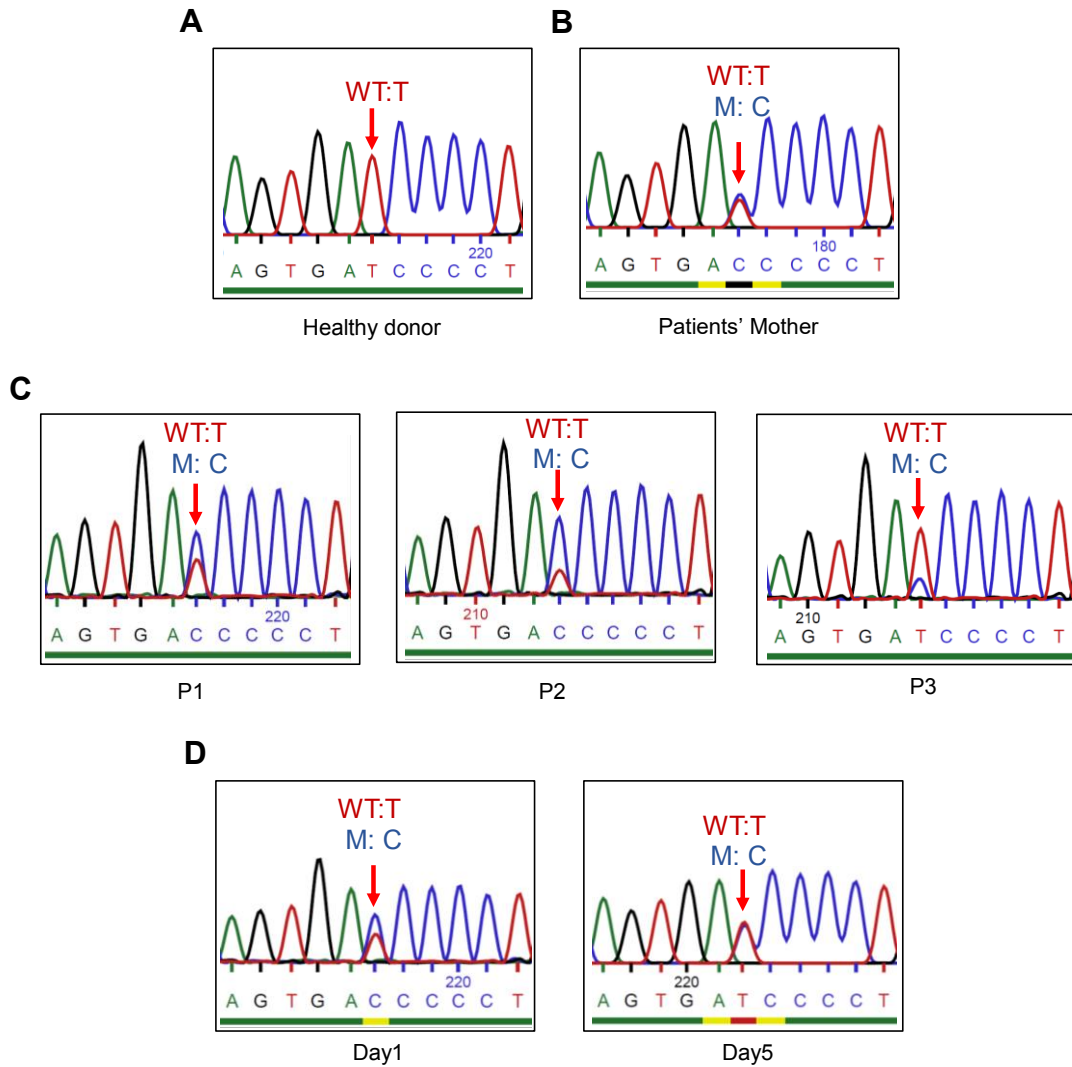


**Figure 4.** Sanger sequence of CD3<sup>+</sup> T cells. Genetic Analysis of T cells based on Sanger sequence of isolated CD3<sup>+</sup> T cells (day0) from (A) healthy donor, (B) patient's mother, and (C) patients. (D) Proliferated CD3<sup>+</sup> T cells from P1 cultured in TexMACS medium supplemented with IL-2 (50 units/mL) were analyzed with Sanger sequencing on day1 (the mutant sequence was 64% on day1 reduced to 47% on day5). The nucleotide T outlined arrow is wild-type (WT) and C is mutant (M). (A-C cited (Hou et al., 2021), D cited (Hou et al., 2022)).

### 3.3 Characterization analysis

To clarify the characteristics of this novel mutation in *IL2RG*, detections of lymphocytes percentage, IL-2R $\gamma$  expression, and CD3<sup>+</sup> T-cell proliferation were implemented.

#### 3.3.1 Inverted CD4<sup>+</sup>/CD8<sup>+</sup> ratio

Compared to healthy donors, patients had inverted CD4<sup>+</sup>/CD8<sup>+</sup> ratio with a lower percentage of CD4<sup>+</sup> T cells ( $p^{**} < 0.01$ ) and a higher frequency of CD8<sup>+</sup> T cells ( $p^{***} < 0.001$ ), while had similar levels of CD3<sup>+</sup>, CD19<sup>+</sup>, and CD56<sup>+</sup> cells (**Figure 5**).

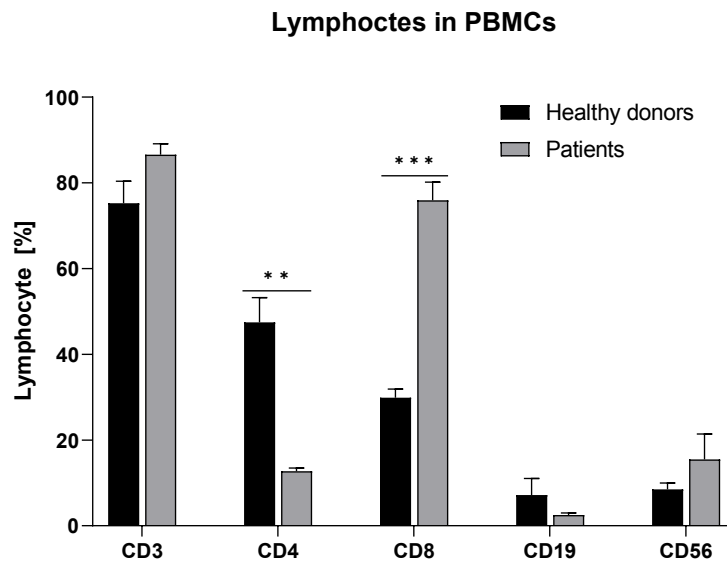


**Figure 5.** Lymphocytes percentage in PBMCs. PBMCs isolated from peripheral blood of healthy donors and patients were detected by flow cytometry by staining with CD3, CD4, CD8, CD19, CD56 antibodies. Bars represent mean  $\pm$  SEM from three biologically independent experiments (N=3). Patients had low CD4<sup>+</sup> cells (\*\*  $p < 0.01$ , unpaired t test) and more CD8<sup>+</sup> cells (\*\*\*)  $p < 0.001$ , unpaired t test), compared to healthy donors, which led to the inverted CD4<sup>+</sup>/CD8<sup>+</sup> ratio. (Hou et al., 2021)

#### 3.3.2 Normal expression of IL-2R $\gamma$

Lymphocyte subsets of CD3<sup>+</sup>, CD4<sup>+</sup>, CD8<sup>+</sup>, CD19<sup>+</sup> and CD56<sup>+</sup> cells of patients expressed IL-2R $\gamma$  at similar levels to the healthy donors (**Figure 6**).

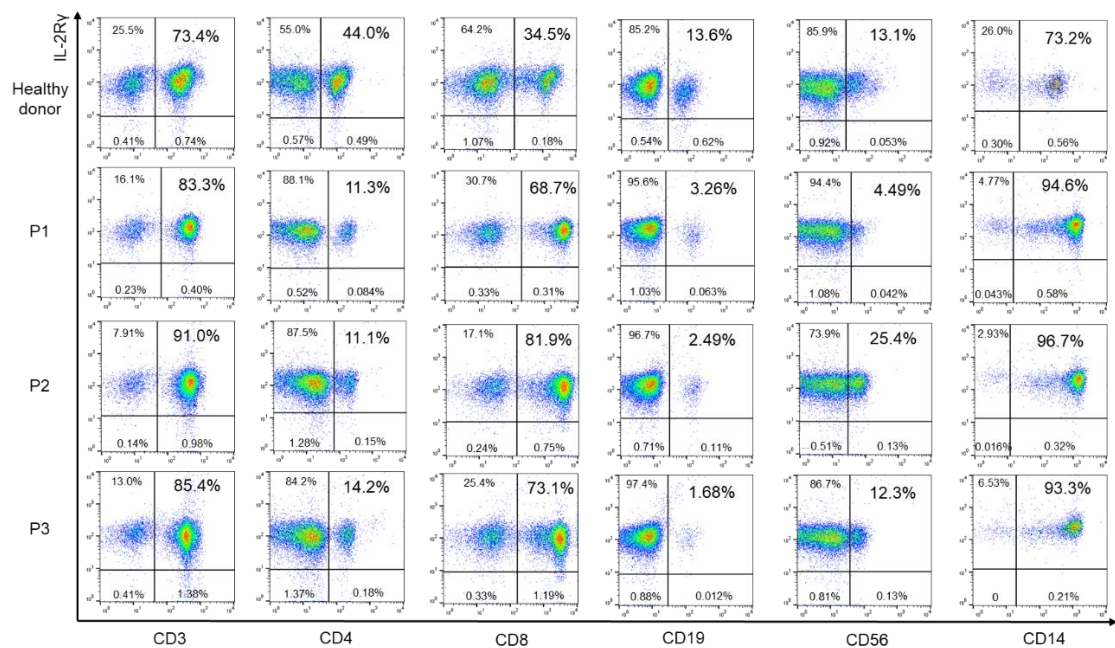


**Figure 6.** IL-2R $\gamma$  expression. IL-2R $\gamma$  was fully expressed in lymphocyte subsets of three patients. PBMCs isolated from three patients and healthy donors (N=3, only one healthy donor is shown here) were stained with CD132-PE antibody and corresponding antibodies of lymphocyte subpopulations. Expression of IL-2R $\gamma$  was detected by flow cytometry and analyzed by FlowJo software. (Hou et al., 2021)

### 3.3.3 Impacted proliferation of CD3<sup>+</sup> T cells

CD3<sup>+</sup> T cells of patients did not proliferate *in vitro* in culture with TexMACS medium supplemented with IL-17 (10 ng/mL) plus IL-15 (5 ng/mL) (**Figure 7.A**), but showed similar proliferation as that of healthy donors when cultured in medium supplemented with IL-2 (50 units/mL) (**Figure 7.B**).

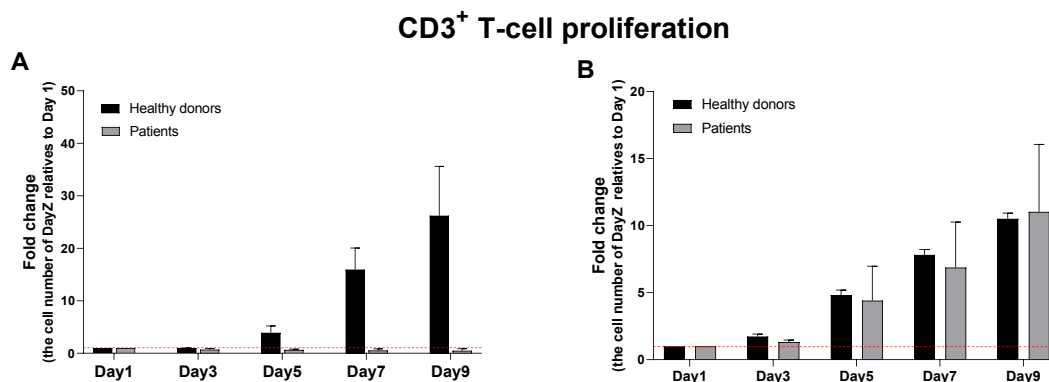
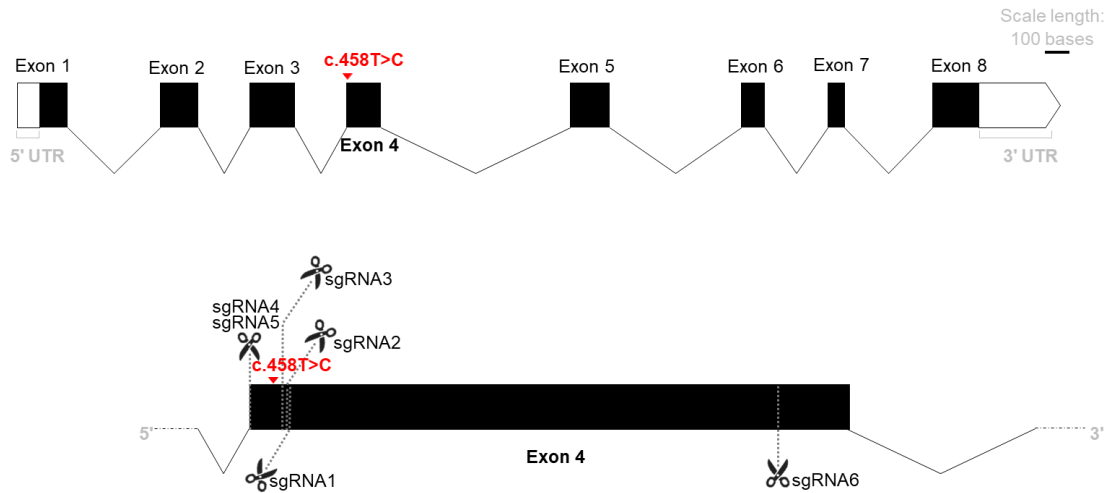


**Figure 7.** Comparison of proliferation of CD3<sup>+</sup> T-cell between patients and healthy donors. Bars with mean  $\pm$  SEM represent the fold-change of cell proliferation as the ratio of cell number between the counting days and day1. All of cells were activated by TransAct. **(A)** Patients' cells (N=3) cannot proliferate (the fold-change is less than 1, marked by the red threshold line) when they were stimulated by IL-7 (10 ng/ml) and IL-15 (5 ng/ml) in TexMACS medium, while the cells of healthy donors (N=3) proliferated considerably. **(B)** When the cells were cultured in the medium with 50 units/mL of IL-2, a similar proliferation rate of cells was observed between patients (N=2, P1 and P2) and healthy donors (N=2). (Hou et al., 2021)

### 3.4 Gene editing by CRISPR/Cas9-ssODN approach

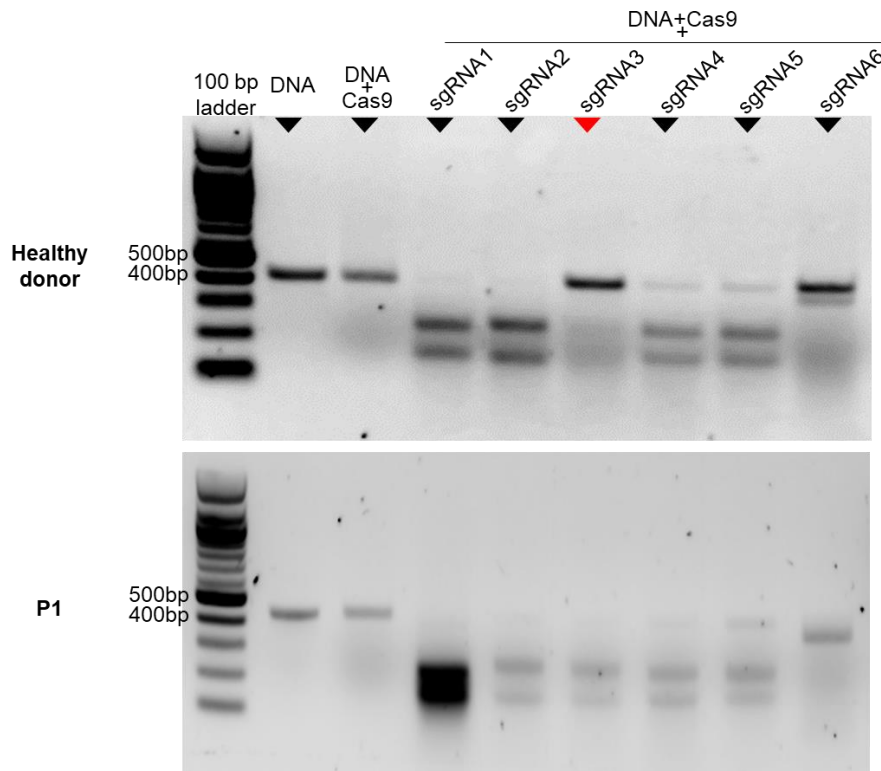
#### 3.4.1 sgRNAs screening for targeting *IL2RG* locus

Considering the mosaicism of CD3<sup>+</sup> T cells due to revertant *IL2RG* mutation, 6 different sgRNAs were designed. The sgRNA1 and sgRNA5 were expected to work only on wild-type sequence, sgRNA2 and sgRNA6 were for both wild-type and mutant and sgRNA3 and sgRNA4 were designed to target only the mutant sequence. Notedly, sgRNA3 was designed with a PAM variation to avoid re-cutting the corrected or wild-type sequence. **(Table 9.1, Figure 8)**



**Figure 8.** Scheme of *IL2RG* gene. *IL2RG* *c.458T>C* mutation is on Exon4. The cutting sites of all 6 designed sgRNAs are presented. sgRNA1 and 5 target wild-type sequence, sgRNA3 and 4 target mutant sequence, and sgRNA2 and 6 target both sequences. (The image was created in Exon-Intron Graphic Maker (<http://wormweb.org/exonintron>) and modified in PowerPoint.)

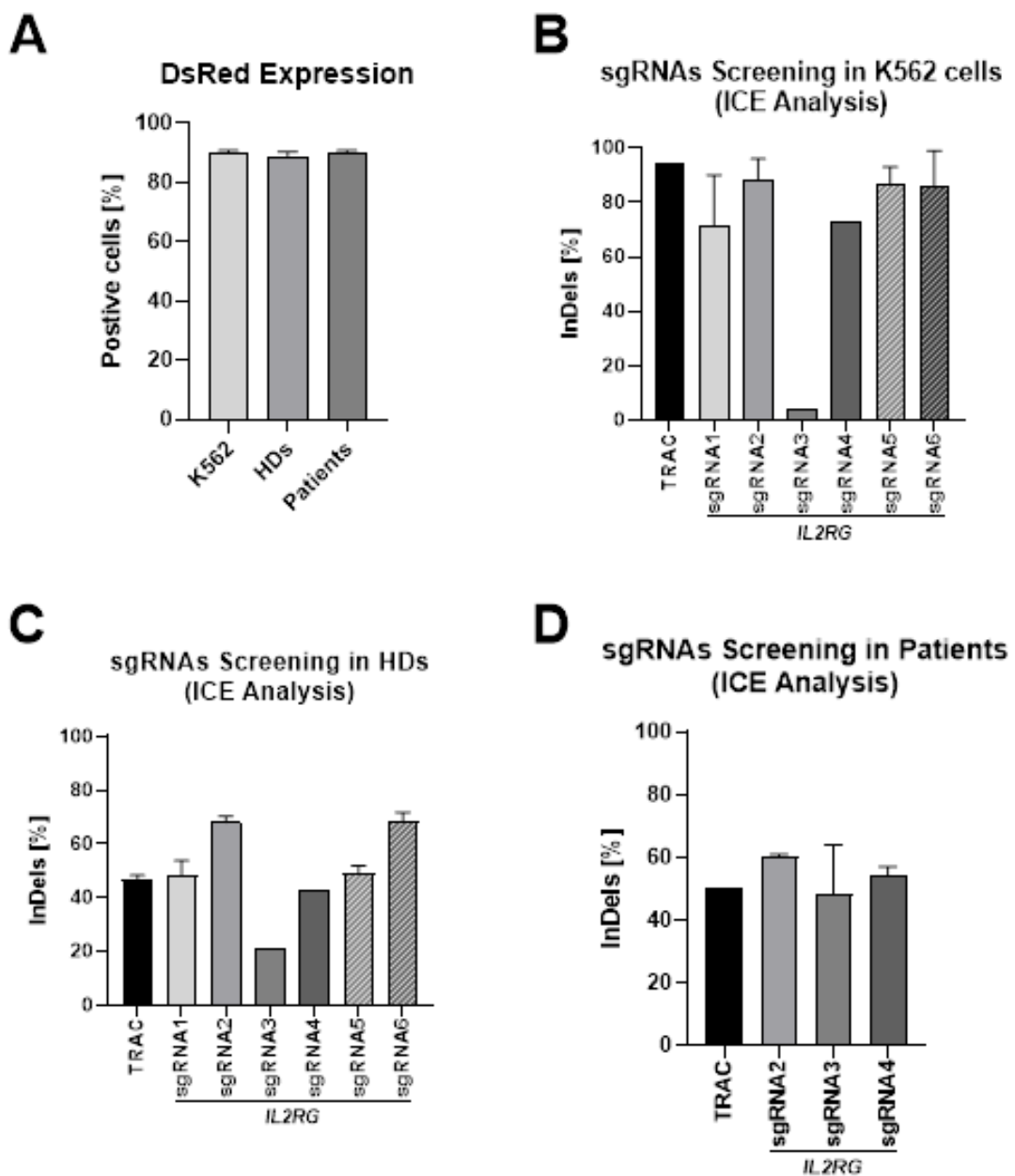
To select suitable sgRNA for correcting the mutation, the cutting efficiency of synthesized sgRNAs was validated by *in vitro* CRISPR/Cas9 cutting assay. As depicted in **Figure 9**, only sgRNA3 worked differently between P1 and the healthy donor since it did not cut the wild-type sequence.



**Figure 9.** *In vitro* CRISPR/Cas9 cutting assay. Amplified DNA (409 bp) was incubated with the RNP complex (respective sgRNAs and Cas9) and the potential cutting visualization (bands with 246bp and 163bp for sgRNA1, 251bp and 158bp for sgRNA2, 250bp and 159bp for sgRNA3, 243bp and 166bp for sgRNA4, 243bp and 166bp for sgRNA5, 364bp and 45bp for sgRNA6) was analyzed in an agarose gel after two hours of incubation. sgRNA1,2,4,5,6 similarly cut the target DNA amplicon of both healthy donor and P1, while sgRNA3 only worked for the DNA of P1. (Hou et al., 2022)

Next, to detect the knock-out capability of sgRNAs using CRISPR/Cas9 system, the sgRNA screening was performed in K562 and CD3<sup>+</sup> T cells. DsRed mRNA was transfected as a reporter of transfection efficiency and its expression was up to 90% of K562 and CD3<sup>+</sup> T cells (**Figure 10.A**). In K562 cells, all sgRNAs produced more than 70% indels frequency, except sgRNA3 (4% indels) (**Figure 10.B**). Screening of sgRNAs in the T cells of healthy donors reported indels frequencies of 21% for gRNA3 and up to 72% for the other sgRNAs (**Figure 10.C**). Patients' T cells were transfected with sgRNA2 (efficient in K562 and healthy donors' T cells), sgRNA3 and sgRNA4 (targeting the mutant sequence) in the following experiments. These sgRNAs achieved 32% to 64% of indels

frequencies (**Figure 10.D**). In all steps, *TRAC* sgRNA (50%-95% indels generation) was transfected to cells as the control sample for knock-out efficiency. Moreover, the proliferation of transfected healthy donors' T cells with RNP complex (*IL2RG* sgRNAs and Cas9) was evaluated. On day 5 post-electroporation, the proliferation of transfected cells decreased significantly compared to non-transfected cells ( $p < 0.0001$ ), however there was no significant reduction in the proliferation of cells transfected with *TRAC* sgRNA (**Figure 10.E**).



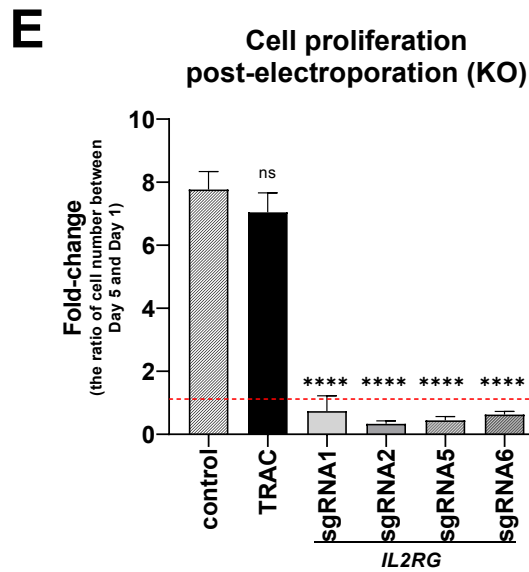


**Figure 10.** Screening sgRNAs in K562 and CD3<sup>+</sup> T cells of healthy donors and patients. Bars represent mean  $\pm$  SEM in two or three independent biological experiments. **(A)** DsRed protein expression was detected 24h post-transfection by flow cytometry as 90% in K562 and T cells. **(B)** sgRNA screening in K562 cells (n=2). All sgRNAs led to more than 70% indels frequency, except sgRNA3 (4%). **(C)** sgRNA screening in T cells of healthy donors (N=3). sgRNA3 generated 21% indels rate whereas the rest of sgRNAs generated more than 60% indels. **(D)** sgRNA screening in T cells of patients (N=2, P1 and P2). sgRNAs induced 32-64% indels formation. **(E)** The proliferation rate of transfected T cells (healthy donors, N=3) is calculated according to the fold-change (ratio) of cell number between day 5 and day 1 post-electroporation. Compared to non-transfected cells, the proliferation rate reduced significantly in cells transfected with *IL2RG* sgRNAs and Cas9 (\*\*\*\* $p < 0.0001$ , Ordinary one-way ANOVA test) but not in cells transfected with *TRAC* sgRNA and Cas9. (Hou et al., 2022)

### 3.4.2 Inducing the *IL2RG* c.458T>C mutation in K562 and T cells

To determine whether our CRISPR/Cas9-ssODN method can modify the *IL2RG* gene at position c.458, we first generated the *IL2RG* c.458T>C mutation in K562 and healthy donors' T cells with two ssODNs carrying the mutant nucleotide. SsODN1 contains the mutant nucleotide (c.458C), whereas ssODN2 carries this mutant nucleotide as well as a silent CRISPR/Cas9-blocking mutation (c.459A) improving editing efficiency (Paquet et al., 2016, Medley et al., 2022). DsRed control samples of K562 and T cells showed 96% expression of DsRed (**Figure 11.A**). In samples transfected with RNP-ssODN, the indels

frequencies were 78-84% in K562 cells and 35-55% in T cells (**Figure 11.B**). Sanger sequencing detected the mutant nucleotides (c.458T>C and c.459C>A) in transfected K562 (**Figure 11.C**) and T cells (**Figure 11.D**). ICE research assessed HDR efficiency as 3.5%±1.5% in K562 cells and 15.0±5.7% in T cells (**Figure 11.E**).

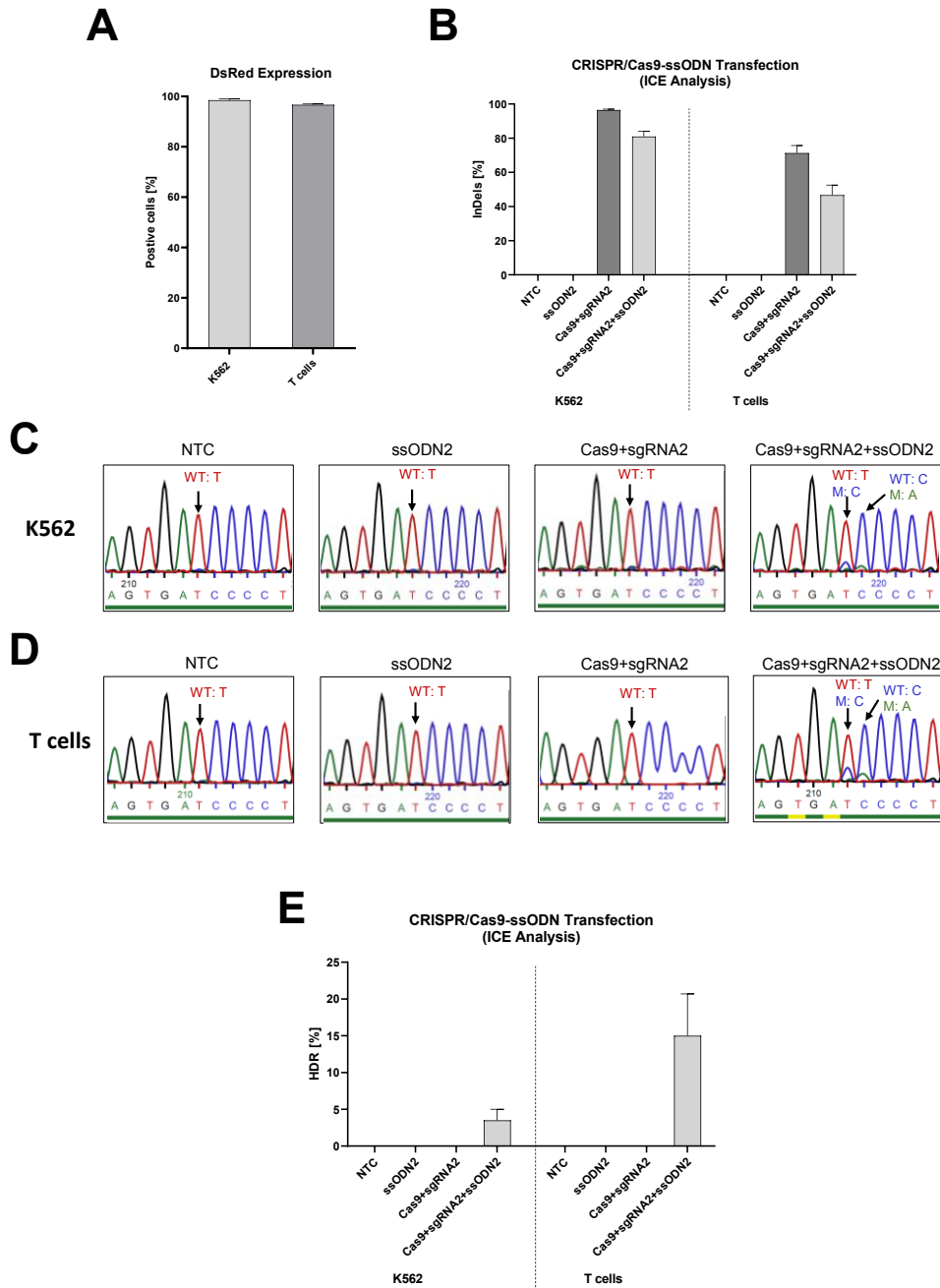


**Figure 11.** CRISPR/Cas9-ssODN strategy for inducing mutation (c.458C>T) in K562 and healthy donors' T cells. Transfection of RNP (*IL2RG* sgRNA2 and Cas9)-ssODN2 was

performed to generate *IL2RG* mutation in K562 (N=2) and healthy donors's T cells (N=3). **(A)** DsRed was expressed in more than 96% of K562 and T cells control samples. **(B)** The frequencies of indels was 96-97% (RNP transfection) and 78-84% (RNP-ssODN transfection) in K562 cells; 66-80% (RNP transfection) and 35-54% (RNP-ssODN transfection) in T cells. Sanger sequencing results of **(C)** K562 and **(D)** T cells transfected with RNP-ssODN showed induced mutant nucleotides of c.458C (targeting inducing mu-tant base) and c.459A (silent blocking mutation). **(E)** HDR efficiency quantified by ICE analysis based on Sanger sequencing showed  $3.5\pm 1.5\%$  HDR in K562 cells and  $15.0\pm 5.7\%$  HDR in T cells. Mean  $\pm$  SEM of biologically independent experiments are shown. (Hou et al., 2022)

### **3.4.3 Correcting the *IL2RG* c.458T>C mutation in mosaic T cells of patients**

To correct the *IL2RG* c.458T>C mutation in mosaic T cells, two ssODNs carrying the wild-type nucleotide (c.458T) were designed. Cells were transfected with the RNP complex (Cas9 with sgRNA3 or sgRNA4) and ssODN (ssODN3 or ssODN4). Up to 90% of cells expressed DsRed in the DsRed transfected control sample (**Figure 12.A**), and 26-72% of indels frequencies were detected in cells transfected with RNP-ssODN (**Figure 12.B**). However, it was not possible to achieve a higher frequency of wild-type nucleotide in modified T cells than the unedited (**Figure 12.C**), which was further validated by ICE and ddPCR analysis (data not shown).

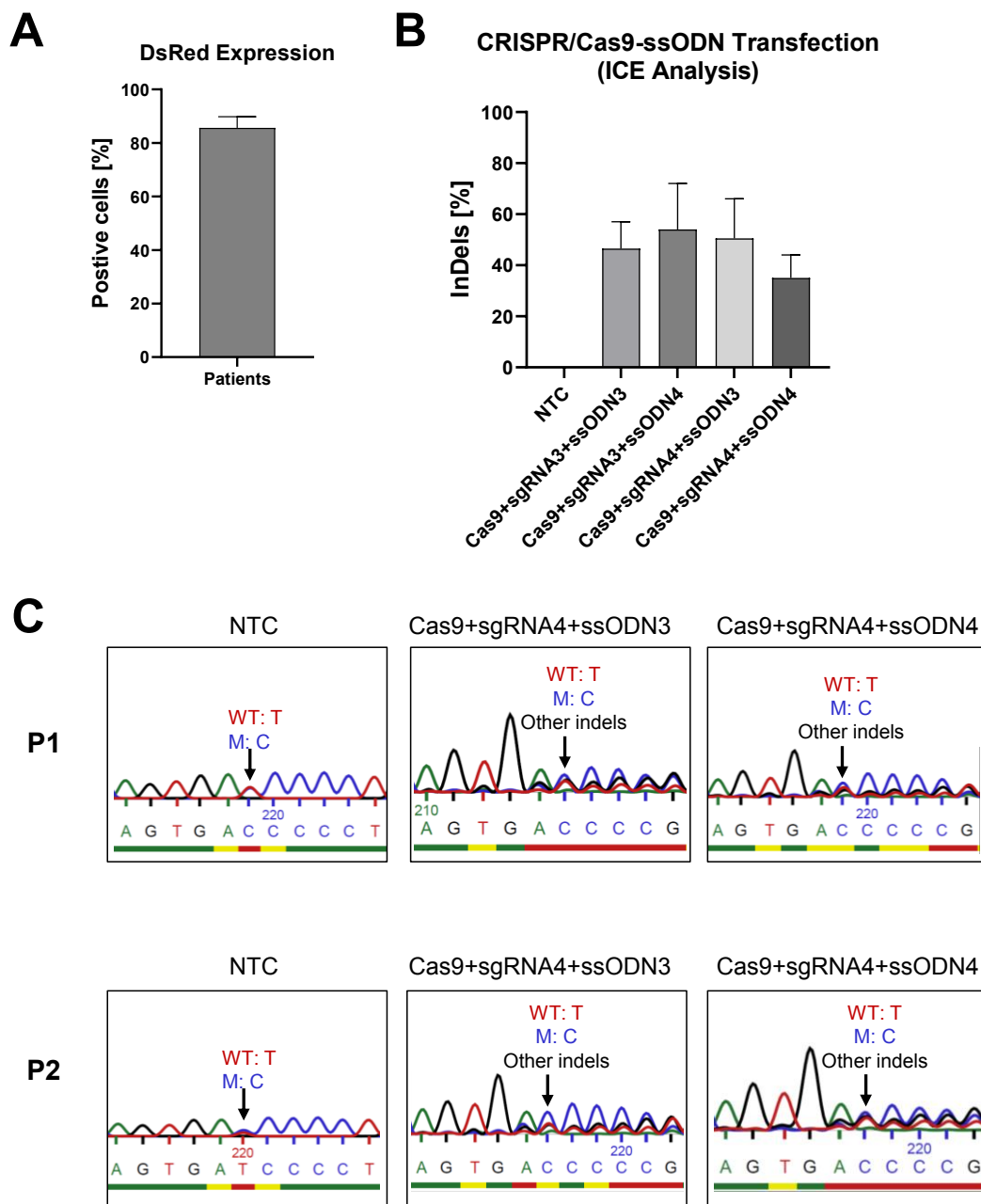


**Figure 12.** CRISPR/Cas9-ssODN transfection in mosaic T cells of patients to correct the *IL2RG* c.458T>C mutation. T cells of patients (N=2, P1 and P2) were transfected with RNP (*IL2RG* sgRNA3/4 and Cas9)-ssODN3/4 to correct the *IL2RG* c.458T>C mutation. **(A)** DsRed mRNA was expressed in up to 90% of cells. **(B)** The indels frequency of edited samples with different RNPs and ssODNs was 26%-72%. Mean  $\pm$  SEM of biologically independent experiments are shown. **(C)** The Sanger sequencing of non-transfected and transfected T cells with Cas9, sgRNA4 and ssODN3/4 of P1 and P2. (Hou et al., 2022)

### 3.5 Gene editing by prime editing strategy

#### 3.5.1 mRNA transcription of PE2 and PE2-GFP plasmids

After performing the maxipreparation, the linearization of PE2 and PE2-GFP plasmids was confirmed by gel electrophoresis (**Figure 13.A**). The *in vitro* transcribed mRNA from both plasmids was synthesized (**Figure 13.B**).

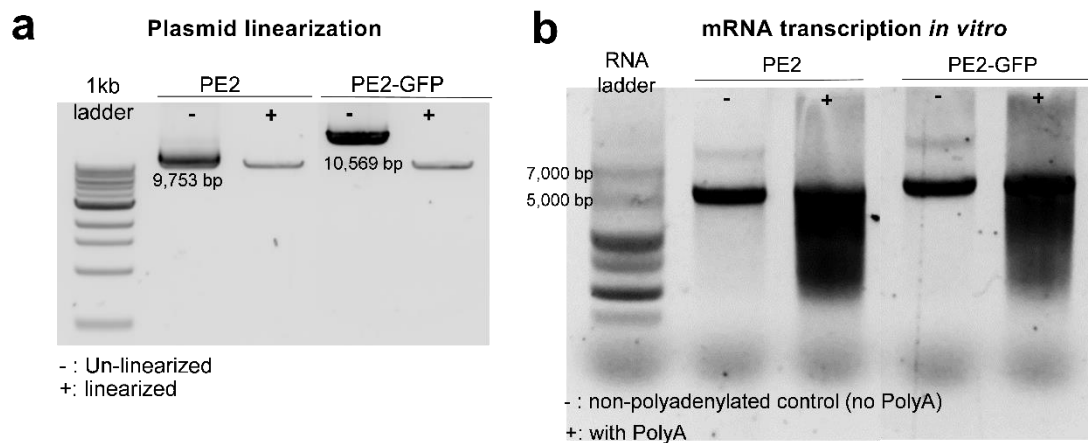


**Figure 13.** Gel visualization of (A) linearized plasmids and (B) synthesized mRNA *in vitro*. (Hou *et al.*, 2022)

#### 3.5.2 Inducing the *IL2RG* c.458T>C mutation in K562 and T cells

To evaluate whether the prime editing strategy can achieve the single nucleotide substitution in the *IL2RG* gene, we first designed pegRNA1 carrying the *IL2RG* c.458T>C variation (**Figure 14**), then transfected PE2/PE2-GFP mRNA and pegRNA into K562 and healthy donor T cells to induce the point mutation.

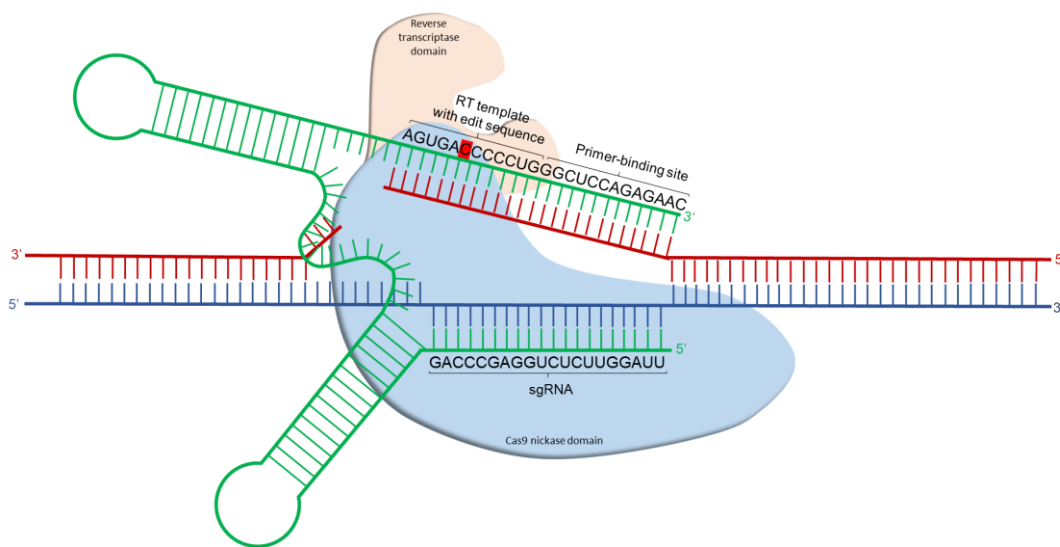


**Figure 14.** Scheme of pegRNA1. The pegRNA1 was designed to introduce the *IL2RG* c.458T>C mutation by PegFinder software online. It contains the sgRNA, RT template with edit sequence (c.458C), and primer binding site (PBS).

24 hours after transfection, up to 88% of K562 cells and 91% of T cells expressed DsRed in control samples transfected with DsRed mRNA, whilst 41-62% of K562 cells and 47-76% of T cells expressed GFP in transfected samples with PE2-GFP mRNA and pegRNA (**Figure 15**).

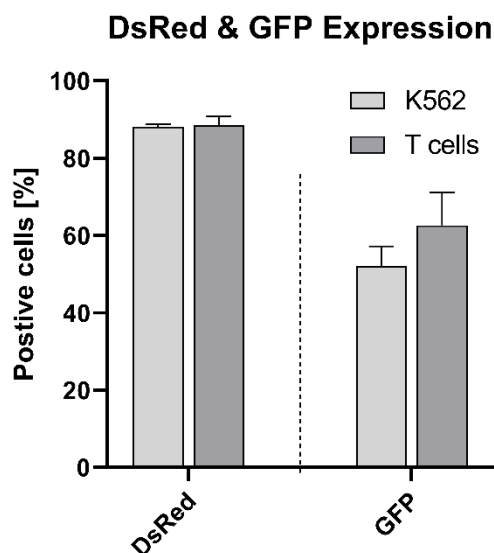


**Figure 15. DsRed and GFP expression.** Up to 88% of K562 cells (N=2) and 91% of T cells (N=3) expressed DsRed in DsRed transfected control samples. 41-62% of K562 cells (N=2) and

47-76% of T cells (N=3) expressed GFP in transfected samples with PE2-GFP mRNA-pegRNA. (Hou et al., 2022)

In K562 cells, Sanger sequencing identified the induced mutation (*IL2RG* c.458T>C) (**Figure 16.A**). RFLP analysis presented the 222bp band for this mutation in transfected cells (**Figure 16.B**). ICE analysis showed  $26.5\pm 2.5\%$  induced mutation in PE2-mRNA and pegRNA transfected cells and  $29.0\pm 1.0\%$  in PE2-GFP mRNA and pegRNA transfected cells (**Figure 16.C**). ddPCR analysis verified the generated mutation. The frequency of the induced mutant nucleotide was  $28.0\pm 3.0\%$  in PE2 mRNA and pegRNA and  $27.5\pm 1.5\%$  in PE2-GFP mRNA and pegRNA transfected cells in ddPCR (**Figure 16.C**).

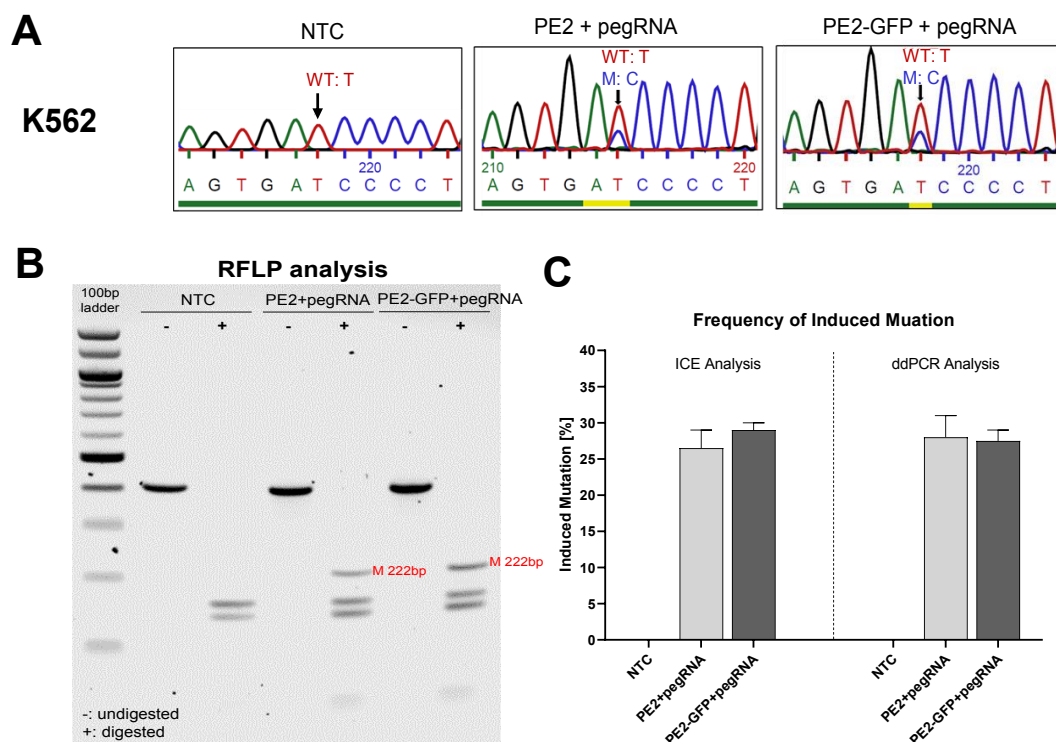


**Figure 16.** Prime editing in K562 to induce the *IL2RG* c.458T>C mutation. (**A**) PE2 mRNA-pegRNA and PE2-GFP mRNA-pegRNA transfected cells showed the induced mutant base c.458C. (**B**) RFLP analysis showed the band with the expected size (222bp) after digestion of PCR product (409bp) by *DpnII* enzyme for the mutant sequence in PE-pegRNA transfected samples. (**C**) The frequency of induced mutation was evaluated by ICE and ddPCR analysis:  $26.5\pm 2.5\%$  (PE2 mRNA-pegRNA) and  $29.0\pm 1.0\%$  (PE2-GFP mRNA-pegRNA) by ICE analysis;

28.0±3.0% (PE2 mRNA-pegRNA) and 27.5±1.5% (PE2-GFP mRNA-pegRNA) by ddPCR analysis. Mean ± SEM of biologically independent experiments are provided (N=2). (Hou et al., 2022)

Furthermore, the same mutation was induced into the T cells of healthy donors. Likewise, the induced mutant nucleotide was identified by Sanger sequence (Figure 17.A) and RFLP analysis (Figure 17.B). ICE analysis quantified the frequency of induced mutation as 16.7±8.4% in PE2 mRNA and pegRNA transfected cells and 21.0±4.0% in PE2-GFP mRNA and pegRNA transfected cells. ddPCR analysis measured the rate of this mutation as 13.1±3.0% in PE2 mRNA and pegRNA transfected cells and 18.0±5.3% in PE2-GFP mRNA and pegRNA transfected cells (Figure 17.C).

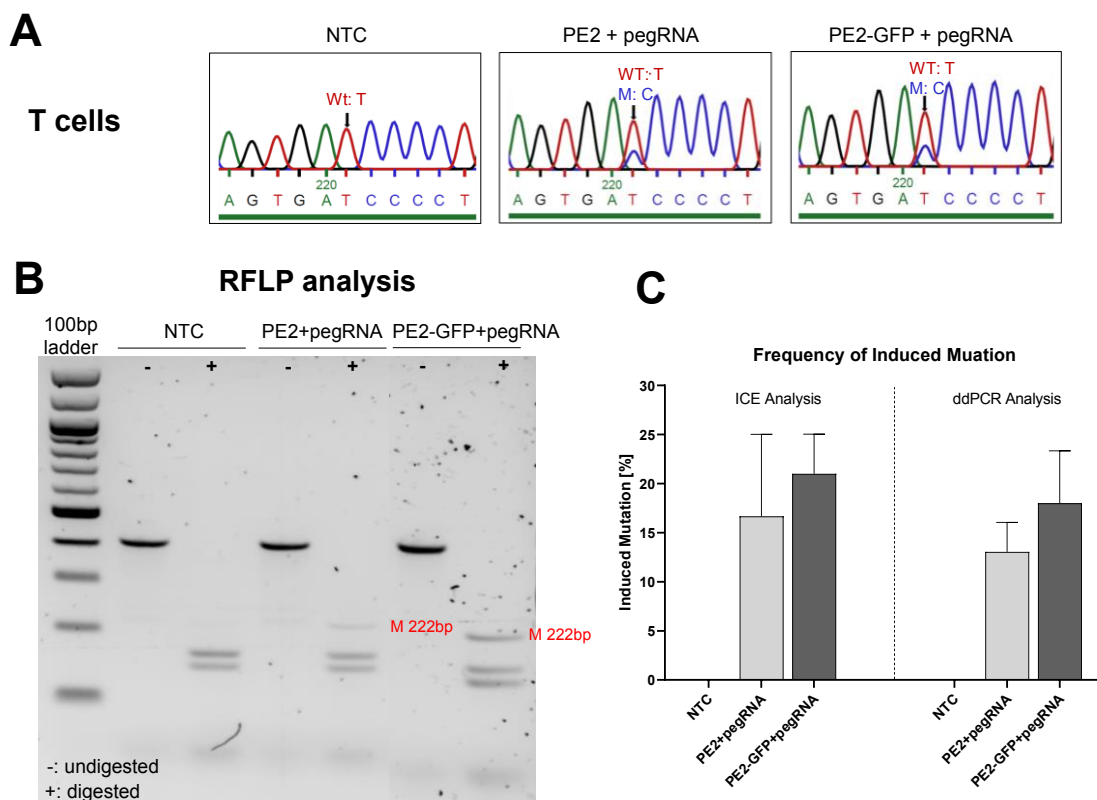


**Figure 17.** Prime editing in T cells of healthy donors to induce the *IL2RG* c.458T>C mutation. (A) PE2 mRNA-pegRNA and PE2-GFP mRNA-pegRNA transfection samples showed the induced mutant base c.458C. (B) RFLP analysis revealed the mutant generation in the edited samples with PE-pegRNA. (C) The frequency of induced mutation was 16.7±8.4% (PE2 mRNA-

pegRNA) and 21.0±4.0% (PE2-GFP mRNA-pegRNA) by ICE analysis and 13.1±3.0% (PE2 mRNA-pegRNA) and 18.0±5.3% (PE2-GFP mRNA-pegRNA) by ddPCR analysis. Mean ± SEM of biologically independent experiments are provided (N=3). (Hou et al., 2022)

### 3.5.3 Correcting the *IL2RG* c.458T>C mutation in mosaic T cells

After confirming the functionality of this approach, pegRNA2 (**Figure 18**) carrying the wild-type nucleotide (c.458T) was designed to transfect patients T cells with PE2/PE2-GFP mRNA in order to correct the *IL2RG* c.458T>C mutation in mosaic T cells.

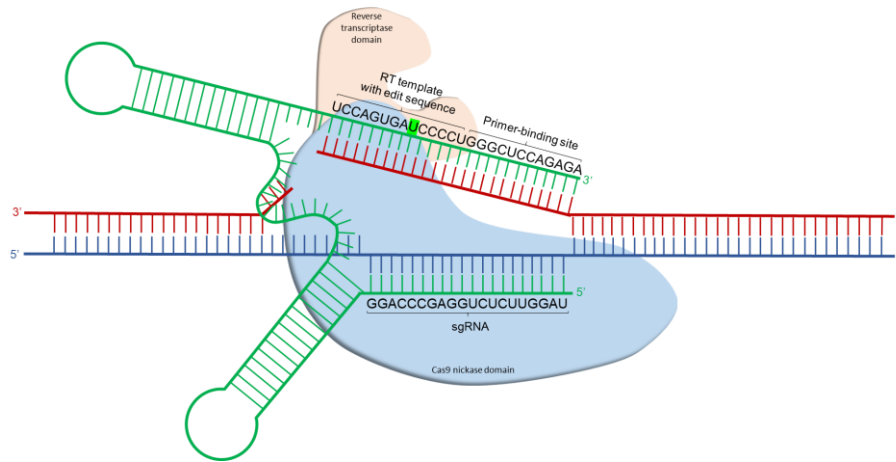


**Figure 18.** Scheme of pegRNA2. The pegRNA2 was designed to correct c.458T>C *IL2RG* mutation by PegFinder software online. It contains the sgRNA, RT template with edit sequence (c.458T), and primer binding site (PBS).

Up to 92% of cells were positive for DsRed expression in control samples transfected with DsRed, whereas 19% expressed GFP in transfected samples with PE2-GFP mRNA and pegRNA2 (**Figure 19.A**). However, Sanger sequencing (**Figure 19.B**), ICE analysis, and ddPCR analysis did not identify correction in patients' mosaic T cells (data not shown).

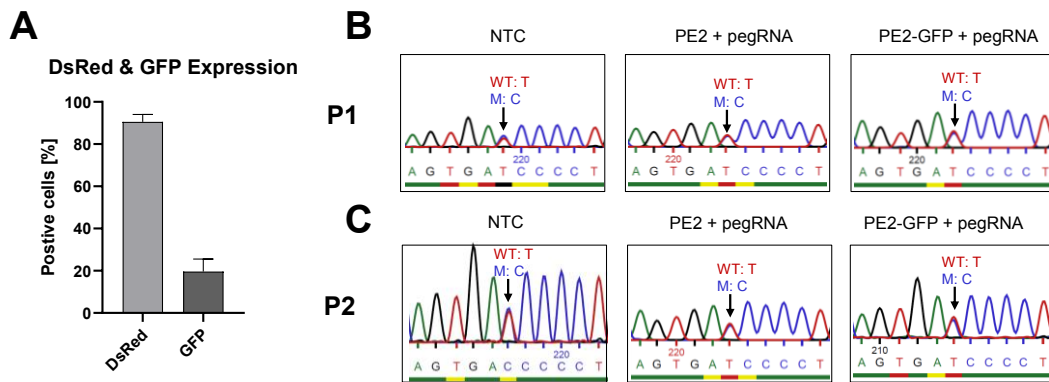


**Figure 19.** Prime editing in mosaic T cells of patients to correct the *IL2RG* c.458T>C mutation. PE (PE2/PE2-GFP mRNA)-pegRNA2 (carrying wild type base c.458T of *IL2RG*) was transfected to edit the *IL2RG* c.458T>C mutation in mosaic T cells of patients (N=2, P1 and P2). **(A)** Up to 92% and 19% of cells expressed the DsRed and GFP respectively. Mean  $\pm$  SEM of biologically independent experiments are shown. The Sanger sequencing did not exhibit significant difference between NTC (non-transfected control) and edited samples (transfected with PE2/PE2-GFP mRNA-pegRNA) in both **(B)** P1 and **(C)** P2. (Hou et al., 2022)

## 4. Discussion

This study discusses the causes of atypical X-SCID in three 20-year-old brothers who carry a novel *IL2RG* variant (c.458T>C, p.Ile153Thr), as well as the application of gene editing, CRISPR/Cas9-ssODN and prime editing strategies, to achieve nucleotide substitution of *IL2RG* gene in K562 and T cells.

### 4.1 Revertant and/or hypomorphic mutation resulting in atypical X-SCID

Three brothers with mild presentation of X-SCID resulting in recurrent chronic respiratory infections and skin warts have been recently described (Hou et al., 2021). CD3<sup>+</sup> T lymphocytes isolated from the peripheral blood of patients contain the mutant and wild-type nucleotides at the same locus of *IL2RG* gene (c.458T>C/T). Excluding the possibility that the wild-type nucleotide was derived from maternal transplantation (Hou et al., 2021), it assumes that the somatic mutation inherited from their mother reverts to the wild type, which is called revertant mutation. The revertant mutation can happen independently among siblings (Ban et al., 2014), but all three brothers here have the reversion only in T-cell populations (Hou et al., 2021) which suggests that the revertant mutation occurs under an unidentified but regular mechanism.

Revertant mutation, also known as "back mutation", is an inherited somatic mutation that reverts back to the wild type, resulting in somatic mosaicism (Aluri and Cooper, 2021, Revy et al., 2019). The reversion could partially or fully compensate for the impairment caused by the initial mutation (Aluri and Cooper, 2021). The revertant cells may gain a proliferative advantage over mutant cells, depending on a variety of parameters, such as the cell lineages and differentiation stages in which the reversion occurs, the lifespan of revertant cells, the characters of the mutant gene, as well as the extrinsic stimulations (Kuijpers et al., 2013, Revy et al., 2019, Palendira et al., 2012). This study showed that the IL-2R $\gamma$  expressed in mosaic CD3<sup>+</sup> T cells of patients equivalently to healthy donors, and STAT5 phosphorylation in CD4<sup>+</sup> and CD8<sup>+</sup> T cells was stimulated similar to healthy controls by high concentrations of IL-2/7

and 15 (Hou et al., 2021), implying that the revertant mutation partially or completely reduces the deficiency of the original mutation. Additionally, the frequency of mutant nucleotide decreased in CD3<sup>+</sup> T cells of P1 with culture days *in vitro*, whilst the frequency of wild-type sequence was increased, which indicates the cells with revertant mutation have an advantage of proliferate. According to the previous reports, the revertant mutation occurs more frequently in T-cell populations of patients with X-SCID (Stephan et al., 1996, Kawai et al., 2012, Kuijpers et al., 2013, Kury et al., 2020, Okuno et al., 2015, Speckmann et al., 2008, Hsu et al., 2015), which may be explained as:

- Easily accessible, rapidly expanding and long-lasting cells are the most potential for observing revertant mutation. (Revy et al., 2019, Hou et al., 2021). While T-cell lineage satisfies these requirements, particularly long-persisting memory T-cells (TSCM) with the extensive capacity for division and self-renewal are the most suitable candidates (Gattinoni et al., 2017).
- The revertant mutation in the T-cell lines offers selection advantages in activation and proliferation, but not in other cell types. This difference in X-SCID may be related to the following: balanced expansion of T-cell when the lymphocytes reduce, cross-functionality of genes for T-cell proliferation, and sustained antigen-specific responses (Revy et al., 2019, Miyazawa and Wada, 2021).

In addition, in terms of the molecular analysis, the amino acid at position 153 in the IL-2R protein is positioned on the cytokine-binding surface of the extracellular domain (Wang et al., 2005). The wild-type amino acid, isoleucine (Ile), at this site is critical to a  $\beta$ -sheet conformation of IL-2R $\gamma$ , and its subchain is not extremely active but takes part in the ligand recognition (**Figure 20.A**). Substitution of isoleucine with threonine (Thr) with isoleucine could maintain the  $\beta$ -sheet motif, due to the adoptable conformations from the main chain being restricted by the two non-hydrogen substituents attached to the beta carbon (**Figure 20.B**) which is similar to isoleucine. To a certain extent, we could conclude that the mutation of p.Ile153Thr has a slight influence on the protein

tertiary structure of IL-2R $\gamma$ . Furthermore, the *IL2RG* p.Ile153Thr is considered as benign mutation by two web-applications (PolyPhen-2: <http://genetics.bwh.harvard.edu/pph2/> ; JCVI: [http://provean.jcvi.org/protein\\_batch\\_submit.php?species=human](http://provean.jcvi.org/protein_batch_submit.php?species=human) ) for prediction of functional effects of human nsSNPs.

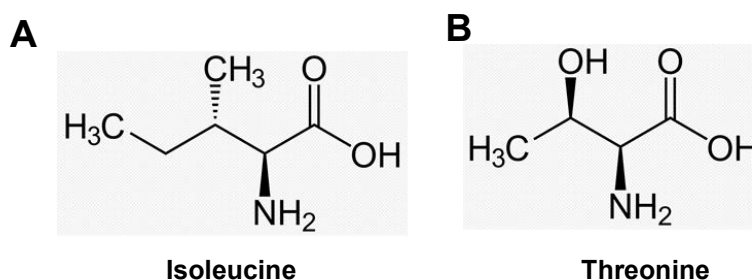


**Figure 20.** The structure of Isoleucine (**A**) and Threonine (**B**). (The images were adopted from <https://pubchem.ncbi.nlm.nih.gov/compound/>)

Besides, patients' CD3<sup>+</sup> T cells did not expand in culture medium supplemented with exogenous IL-7 and IL-15, but they proliferated with addition of IL-2 *in vitro*. This observation demonstrates that cells require exogenous IL-2 to maintain their proliferation and survival as they might be unable to generate enough IL-2 on their own. Additionally, the CD4<sup>+</sup>/CD8<sup>+</sup> ratio in the lymphocyte populations of patients was inverted. According to Kuijpers et al. (Kuijpers et al., 2013), one possible explanation is that CD4<sup>+</sup> T cells exhibit a slower cellular proliferation than CD8<sup>+</sup> T cells since CD8<sup>+</sup> T cells have a higher antigen-driven. These observations indicate that the function of patients' T cells is slightly impaired by *IL2RG* c.458T>C mutation and/or is partly reconstituted due to the compensatory revertant mutation. Besides, IL-2R $\gamma$  expresses normally not only in T cells with revertant mutation but also in B and NK cells without reversion, and P1 has slight elevated IgG1, low IgG2, and undetectable IgG4 (Hou et al., 2021) (only P1 is followed up with the evaluation of immunophenotype) which means B and NK cells of patients have minor defects.

Therefore, it suggests that revertant and/or hypomorphic *IL2RG* c.458T>C mutation results in the mild phenotype of patients with X-SCID in our study.

## 4.2 Gene editing for nucleotide substitution of *IL2RG* in K562 and T cells

Although somatic revertant mosaicism have been considered as a “natural therapy” for improving the clinical conditions of patients (Stephan et al., 1996, Kawai et al., 2012, Hsu et al., 2015, Kuijpers et al., 2013, Kury et al., 2020, Speckmann et al., 2008), some of the patients present more severe symptoms with age (Okuno et al., 2015, Lin et al., 2020). Therefore, gene therapy remains an alternative potential treatment to increase the frequency of corrected cells in somatic reverted mosaicisms.

In some studies, including this study, CRISPR/Cas9-ssODN was utilized as one of the gene therapy techniques owing to its adaptability and simplicity of usage, as well as easy design, quick and economical manufacture of ssODNs (Azhagiri et al., 2021). Even though the CRISPR/Cas9 system is a highly effective method for generating insertions and deletions in the target region, the generation of HDR is relatively low. Because the majority of DSBs are repaired by the NHEJ pathway, resulting in nonspecific insertions, deletions, or other variations (Hsu et al., 2014, Cong et al., 2013). As anticipated, our findings revealed a higher indel frequency than HDR in edited samples with CRISPR/Cas9-ssODN. Certainly, HDR formation is also dependent on the features of ssODNs (such as the length of homology arms, size, orientation, and blocking mutation), the type of modified cells, and gene locus (Cong et al., 2013, Okamoto et al., 2019, Antony et al., 2018). Hence, it is necessary to optimize ssODNs to increase HDR efficiency.

This study also employed prime editing as a safer and potentially more effective technology. Theoretically, 89% of known mutations related to genetic disorders can be modified using prime editing (Anzalone et al., 2019). More advanced generation of prime editing could improve the editing effectiveness for nucleotide substitutions, small insertion, and deletion (Anzalone et al., 2019). Anzalone et al. (Anzalone et al., 2019) used PE2 to generate point mutation at multiple genomic loci in HEK293T cells, achieving an editing efficiency of 1.1-28.1%. Li et al. (Li et al., 2022) inserted point mutations in alpha-synuclein (*SNCA*) gene (A30P) locus in wild-type human pluripotent stem cells (hPSCs)

utilizing PE2 in the forms of plasmid, RNP, and mRNA and achieved around 5%, 1%, and 26.7% editing efficiency, respectively. This result showed that the mRNA format in PE2 system is more effective. Here, using the PE2-pegRNA method for introducing single nucleotide substitution achieved the *IL2RG* c.458T>C mutation with a maximum efficiency of 31% and 26%, respectively, in K562 and healthy donor T cells. This strategy, provides an *in vitro* model for X-SCID disease and would contribute to optimize the similar gene-editing strategy in patient cells. Moreover, compared to the CRISPR/Cas9-ssODN method, prime editing generated more efficiency in inducing *IL2RG* c.458T>C mutation. Consistent with earlier research (Anzalone et al., 2019), Sanger sequencing showed no on-target indels formation in samples edited with prime editing, implying that indels introduction is rare during the prime editing process.

Although it was feasible to complete the nucleotide substitution of *IL2RG* with CRISPR/Cas9-ssODN and prime editing in this work, similar techniques were employed to modify the *IL2RG* c.458T>C mutation in mosaic T cells of patients but it did not increase the frequency of wild-type nucleotide. It is hypothesized that the revertant mutation in mosaic T cells of patients hampers a beneficial result:

- The existence of revertant mutations impairs editing efficiency. The coexistence of wild-type and mutant sequences with only a single nucleotide difference in the targeted region hinders the precision targeting of CRISPR/Cas9 and prime editing systems. In addition, when the frequency of gene editing is low, it is more challenging to determine the modified nucleotide. To accurately quantify the correction efficiency, higher sensitive genotyping methods would be needed (Tsiatis et al., 2010).
- In a mosaic population, the possibility of targeting mutant cells is diminished. The proliferation rate of CD3<sup>+</sup> T cells from patients was significantly lower than that of healthy donors. Genetic analysis of CD3<sup>+</sup> T cells from patients cultured *in vitro* showed that the frequency of mutant sequence decreased over time. These observations demonstrate

that the mutant cells are poorly able to expand *in vitro*. Conversely, cells carrying revertant mutations have a proliferative advantage which is consistent with findings of previous studies (Miyazawa and Wada, 2021, Kuijpers et al., 2013). This reduces the probability of targeting mutant cells with the gene-editing strategy in a heterogeneous population.

The mutagenic outcome in this study suggests that using CRISPR/Cas9-ssODN and prime editing strategies are suitable to modify mutations in the same locus in *IL2RG* gene without reversions in X-SCID patient cells. However, further technical optimization is required to correct mutations in somatic reverted mosaicism background.

### **4.3 The importance of identification of genetic mosaicisms**

In diagnosing genetic disorders, precise identification of mosaicisms should be emphasized. Due to revertant mutations, recognizing defect DNA variations is more difficult in mosaicisms (Aluri and Cooper, 2021). The accurate detection of mosaicism is based on the type of acquired cells (in this instance, only subsets of T cells showed the revertant mutation) and the sensitivity of genotyping methods (Aluri and Cooper, 2021, Biesecker and Spinner, 2013). To determine the existence of reversion in patients with atypical X-SCID, genomic sequencing of multiple immune cell subtypes is recommended. Additionally, more sensitive techniques, such as next-generation sequencing (NGS), quantitative PCR (q-PCR), and ddPCR, should be utilized to determine and quantify mosaicism (Tsiatis et al., 2010). Furthermore, exon sequencing and whole genome sequencing are widely employed to identify pathogenic DNA variants (Tsiatis et al., 2010). Therefore, patients with atypical clinical symptoms of genopathy should be evaluated using a multitude of detecting methods. After a thorough analysis of the detected results, the precise diagnosis and medical management should be offered.

#### **4.4 Limitations of the study**

It requires higher volumes of blood to obtain enough cellular material for proliferation *in vitro* in order to perform a direct genetic modification of T cells from patients, but for ethical reasons, no further investigation was performed. Likewise, hematopoietic stem cells (HSCs) would fit more for gene modification to establish persistent immune reconstitution but patients' HSCs were not collected or employed in the current work for medical ethics. Moreover, gene-editing strategies and editing-efficiency measurements need to be further optimized.

## 4.5 Conclusion

In summary, the X-SCID patients in this study present mild clinical presentation due to the revertant and/or hypomorphic mutation of *IL2RG* gene allowing particular immune reconstruction. As they still have symptoms with the natural correction from the revertant mutation, it was considered to study the potential of gene therapy to increase corrected cells. CRISPR/Cas9-ssODN and prime editing methods were designed and applied to induce the *IL2RG* c.458C>T mutation in K562 and healthy donors' T cells. This *in vitro* model of X-SCID can improve the accurate evaluation of possible progressions and potential treatments of the disease. Based on the results, the strategies failed to increase the frequency of wild-type sequence in mosaic T cells of patients since limited *in vitro* proliferation of mutant cells and the presence of somatic reversion make correcting of the mutant cells in the mosaic population more challenging. Nevertheless, the potential of nucleotide substitution of the *IL2RG* gene by gene therapy, particularly prime editing, could offer an alternative treatment for X-SCID patients without revertant mutations. Additionally, further technological optimizations and developments are required to modify the mutations in somatic mosaicism.

## 5.1 Summary

X-linked severe combined immunodeficiency (X-SCID) is a rare primary immunodeficiency disorder with X-chromosome-linked recessive inheritance, that is caused by the mutations of the interleukin-2 receptor gamma (*IL2RG*) gene. The *IL2RG* gene encodes the interleukin-2 receptor common gamma chain (IL-2R $\gamma$ , also known as  $\gamma$ c). The IL-2R $\gamma$  is essential not only for lymphocyte development and immune function but also for maintaining the structure of the IL-2R complex and the link of intracellular signaling molecules. The mutations of *IL2RG* can result in impaired lymphocytes and deficiency immunity. Some patients of atypical X-SCID present mild syndrome due to hypomorphic or revertant *IL2RG* mutations.

This study describes a novel *IL2RG* variant (c.458T>C, p.Ile153Thr) in three 20-year-old brothers with atypical X-SCID. They had a regular frequency of lymphocytes in peripheral blood but an inverted CD4<sup>+</sup>/CD8<sup>+</sup> ratio. IL-2R $\gamma$  expression was detected commonly in lymphocyte subsets, while their CD3<sup>+</sup> T cell proliferation *in vitro* was impacted. They have occasionally suffered from respiratory infections and skin warts. The mutant and wild-type (the mutation reverted to the wild type) nucleotides at the same site of *IL2RG* gene (c.458T>C/T) were co-exist in their T-cell populations. Despite the observation of somatic revertant mosaicism as a naturally occurring mechanism of gene correction, the patients still exhibit symptoms. Therefore, gene editing offers a potential therapy to increase the frequency of corrected T cells.

Here, advanced genome editing tools, CRISPR/Cas9-ssODN and prime editing, were applied to modify the *IL2RG* gene at the specific locus 458 in exon 4. These two methods were successfully applied to establish an *in vitro* model of X-SCID in K562 cells and healthy donors' T cells to introduce the c. 458T>C mutation in *IL2RG* gene. However, the similar strategies were not able to correct the *IL2RG* c. 458T>C mutation in patients' T cells due to the limited *in vitro* proliferation of mutant cells and the presence of somatic reversion. This study describes that gene editing in a mixed population of mutated and reverted

cells might hinder gene therapy application, and summarizes the main challenges and limitations confronted with. Nevertheless, results of this project implicate the feasibility of precise nucleotide substitution of *IL2RG* gene locus, especially by prime editing. Gene therapy based on CRISPR/Cas9-ssODN and prime editing could provide an alternative treatment for X-SCID patients. Further technology improvement needs to be developed to correct the mutations in somatic mosaicisms.

## 5.2 Zusammenfassung

Die X-linked Severe Combined Immunodeficiency (X-SCID) ist ein seltener, primärer Immundefekt, welcher über eine X chromosomale rezessive Vererbung eine Mutation im Interleukin-2 Rezeptor Gamma (*IL2RG*) Gen verursacht. Das *IL2RG* Gen kodiert für die Common Gamma Kette des Interleukin-2 Rezeptors (IL-2R $\gamma$ , auch als  $\gamma_c$  bezeichnet). Diese spielt eine entscheidende Rolle bei der Entwicklung von Lymphozyten sowie der Funktion des Immunsystems. Die IL-2R $\gamma$  ist zudem beim Erhalt der Struktur des IL-2R Komplexes sowie für intrazelluläre Signalmoleküle und Signalkaskaden von wichtiger Bedeutung. Mutationen im *IL2RG* Gen können zu funktionsbeeinträchtigten Lymphozyten und somit zu Defekten in der Immunantwort führen. Einige Patienten mit atypischer X-SCID weisen aufgrund hypomorpher oder revertanter *IL2RG*-Mutationen ein mildes Syndrom auf.

In dieser Studie wird eine neue *IL2RG*-Variante (c.458T>C, p.Ile153Thr) bei drei Geschwistern mit atypischem X-SCID beschrieben. Sie wiesen eine Normverteilung von Lymphozyten im peripheren Blut, jedoch eine abweichende CD4<sup>+</sup>/CD8<sup>+</sup>-Ratio auf. Die IL-2R $\gamma$ -Expression wurde häufig in Lymphozytensubpopulationen nachgewiesen, die in ihrer CD3<sup>+</sup>-T-Zellproliferation *in vitro* beeinträchtigt waren. Betroffene Patienten litten gelegentlich an Atemwegsinfektionen und Hautwarzen. In T-Zell-Populationen dieser Patienten konnte das gleichzeitige Vorhandensein von mutierten und Wildtyp-Nukleotiden (die Mutation kehrte zum Wildtyp zurück) an derselben Stelle des *IL2RG*-Gens (c.458T>C/T) nachgewiesen werden. Trotz Vorhandenseins von somatisch revertantem Mosaizismus, der einen natürlich vorkommenden Mechanismus der Genkorrektur darstellt, weisen diese Patienten weiterhin Symptome auf. Daher bietet die Genomeditierung eine potenzielle Therapieplattform zur Erhöhung der Frequenz korrigierter T-Zellen.

In dieser Studie wurden CRISPR/Cas9-ssODN und Prime Editing, zwei fortgeschrittene Genomeditierung Methoden eingesetzt, um das *IL2RG*-Gen spezifisch am Locus 458 in Exon 4 zu modifizieren. Diese beiden Methoden

wurden hier erfolgreich angewendet, um ein in vitro Modell zur Einleitung der c. 458T>C-Mutation im *IL2RG*-Gen von X-SCID in K562-Zellen und T-Zellen gesunder Spender zu etablieren. Es war jedoch nicht möglich mit ähnlichen angewandten Methoden die *IL2RG* c. 458T>C-Mutation in T-Zellen von Patienten zu korrigieren, da sich die mutierten Zellen in vitro nur begrenzt vermehren und eine somatische Reversion in diesen vorlag. Folgend wird beschrieben wie das Genomeditierung in einer gemischten Population von mutierten und revertierten Zellen die Anwendung der Gentherapie behindern kann. Des Weiteren werden hier die wichtigsten Herausforderungen und Einschränkungen zusammengefasst. Nichtsdestotrotz deuten Ergebnisse dieses Projekts darauf hin, dass eine präzise Nukleotidsubstitution des *IL2RG*-Genlocus möglich ist, insbesondere durch Prime Editing. Eine Gentherapie, welche auf CRISPR/Cas9-ssODN beruht, könnte eine alternative Behandlung für X-SCID-Patienten in Zukunft darstellen. Weitere technische Verbesserungen sind notwendig um die Mutationen bei Vorliegen eines somatischen Mosaiks korrigieren zu können.

## 6. Bibliography

- ALURI, J. & COOPER, M. A. 2021. Genetic Mosaicism as a Cause of Inborn Errors of Immunity. *J Clin Immunol*, 41, 718-728.
- ANTONY, J. S., DANIEL-MORENO, A., LAMSFUS-CALLE, A., RAJU, J., KAFTANCIOGLU, M., UREÑA-BAILÉN, G., ROTTENBERGER, J., HOU, Y., SANTHANAKUMARAN, V., LEE, J. H., HEUMOS, L., BÖHRINGER, J., KRÄGELOH-MANN, I., HANDGRETINGER, R. & MEZGER, M. 2022. A Mutation-Agnostic Hematopoietic Stem Cell Gene Therapy for Metachromatic Leukodystrophy. *Crispr j*, 5, 66-79.
- ANTONY, J. S., LATIFI, N., HAQUE, A., LAMSFUS-CALLE, A., DANIEL-MORENO, A., GRAETER, S., BASKARAN, P., WEINMANN, P., MEZGER, M., HANDGRETINGER, R. & KORMANN, M. S. D. 2018. Gene correction of HBB mutations in CD34(+) hematopoietic stem cells using Cas9 mRNA and ssODN donors. *Mol Cell Pediatr*, 5, 9.
- ANZALONE, A. V., RANDOLPH, P. B., DAVIS, J. R., SOUSA, A. A., KOBLAN, L. W., LEVY, J. M., CHEN, P. J., WILSON, C., NEWBY, G. A., RAGURAM, A. & LIU, D. R. 2019. Search-and-replace genome editing without double-strand breaks or donor DNA. *Nature*, 576, 149-157.
- AZHAGIRI, M. K. K., BABU, P., VENKATESAN, V. & THANGAVEL, S. 2021. Homology-directed gene-editing approaches for hematopoietic stem and progenitor cell gene therapy. *Stem Cell Res Ther*, 12, 500.
- BAN, S. A., SALZER, E., EIBL, M. M., LINDER, A., GEIER, C. B., SANTOS-VALENTE, E., GARNCARZ, W., LION, T., OTT, R., SEELBACH, C., BOZTUG, K. & WOLF, H. M. 2014. Combined immunodeficiency evolving into predominant CD4+ lymphopenia caused by somatic chimerism in JAK3. *J Clin Immunol*, 34, 941-53.
- BIESECKER, L. G. & SPINNER, N. B. 2013. A genomic view of mosaicism and human disease. *Nat Rev Genet*, 14, 307-20.
- BROOKS, E. G., SCHMALSTIEG, F. C., WIRT, D. P., ROSENBLATT, H. M., ADKINS, L. T., LOOKINGBILL, D. P., RUDLOFF, H. E., RAKUSAN, T. A. & GOLDMAN, A. S. 1990. A novel X-linked combined immunodeficiency disease. *J Clin Invest*, 86, 1623-31.
- BUSTAMANTE OGANDO, J. C., PARTIDA GAYTÁN, A., ALDAVE BECERRA, J. C., ÁLVAREZ CARDONA, A., BEZRODNIK, L., BORZUTZKY, A., BLANCAS GALICIA, L., CABANILLAS, D., CONDINO-NETO, A., DE COLSA RANERO, A., ESPINOSA PADILLA, S., FERNANDES, J. F., GARCÍA CAMPOS, J. A., GÓMEZ TELLO, H., GONZÁLEZ SERRANO, M. E., GUTIÉRREZ HERNÁNDEZ, A., HERNÁNDEZ BAUTISTA, V. M., IVANKOVICH ESCOTO, G., KING, A., LESSA MAZZUCHELLI, J., LLAMAS GUILLÉN, B. A., LUGO REYES, S. O., MORENO ESPINOSA, S., OLEASTRO, M., OTERO MENDOZA, F., POLI HARLOWE, M. C., PORRAS, O., RAMIREZ URIBE, N., REGAIRAZ, L., RIVAS LARRAURI, F., SARACHO WEBER, F. J., GRUMACH, A. S., STAINES BOONE, T., TAVARES COSTA-CARVALHO, B., YAMAZAKI NAKASHIMADA, M. A. & ESPINOSA ROSALES, F. J. 2019. Latin American consensus on the

- supportive management of patients with severe combined immunodeficiency. *J Allergy Clin Immunol*, 144, 897-905.
- CONG, L., RAN, F. A., COX, D., LIN, S., BARRETTO, R., HABIB, N., HSU, P. D., WU, X., JIANG, W., MARRAFFINI, L. A. & ZHANG, F. 2013. Multiplex genome engineering using CRISPR/Cas systems. *Science*, 339, 819-23.
- DE RAVIN, S. S., LI, L., WU, X., CHOI, U., ALLEN, C., KOONTZ, S., LEE, J., THEOBALD-WHITING, N., CHU, J., GAROFALO, M., SWEENEY, C., KARDAVA, L., MOIR, S., VILEY, A., NATARAJAN, P., SU, L., KUHN, D., ZAREMBER, K. A., PESHWA, M. V. & MALECH, H. L. 2017. CRISPR-Cas9 gene repair of hematopoietic stem cells from patients with X-linked chronic granulomatous disease. *Sci Transl Med*, 9.
- DE RAVIN, S. S., WU, X., MOIR, S., ANAYA-O'BRIEN, S., KWATEMAA, N., LITTEL, P., THEOBALD, N., CHOI, U., SU, L., MARQUESEN, M., HILLIGOSS, D., LEE, J., BUCKNER, C. M., ZAREMBER, K. A., O'CONNOR, G., MCVICAR, D., KUHN, D., THROM, R. E., ZHOU, S., NOTARANGELO, L. D., HANSON, I. C., COWAN, M. J., KANG, E., HADIGAN, C., MEAGHER, M., GRAY, J. T., SORRENTINO, B. P., MALECH, H. L. & KARDAVA, L. 2016. Lentiviral hematopoietic stem cell gene therapy for X-linked severe combined immunodeficiency. *Sci Transl Med*, 8, 335ra57.
- DEVKOTA, S. 2018. The road less traveled: strategies to enhance the frequency of homology-directed repair (HDR) for increased efficiency of CRISPR/Cas-mediated transgenesis. *BMB Rep*, 51, 437-443.
- DEWITT, M. A., MAGIS, W., BRAY, N. L., WANG, T., BERMAN, J. R., URBINATI, F., HEO, S. J., MITROS, T., MUÑOZ, D. P., BOFFELLI, D., KOHN, D. B., WALTERS, M. C., CARROLL, D., MARTIN, D. I. & CORN, J. E. 2016. Selection-free genome editing of the sickle mutation in human adult hematopoietic stem/progenitor cells. *Sci Transl Med*, 8, 360ra134.
- DORSEY, M. J., DVORAK, C. C., COWAN, M. J. & PUCK, J. M. 2017. Treatment of infants identified as having severe combined immunodeficiency by means of newborn screening. *J Allergy Clin Immunol*, 139, 733-742.
- FELGENTREFF, K., PEREZ-BECKER, R., SPECKMANN, C., SCHWARZ, K., KALWAK, K., MARKELJ, G., AVCIN, T., QASIM, W., DAVIES, E. G., NIEHUES, T. & EHL, S. 2011. Clinical and immunological manifestations of patients with atypical severe combined immunodeficiency. *Clin Immunol*, 141, 73-82.
- GASPAR, H. B., QASIM, W., DAVIES, E. G., RAO, K., AMROLIA, P. J. & VEYS, P. 2013. How I treat severe combined immunodeficiency. *Blood*, 122, 3749-58.
- GATTI, R. A., MEUWISSEN, H. J., ALLEN, H. D., HONG, R. & GOOD, R. A. 1968. Immunological reconstitution of sex-linked lymphopenic immunological deficiency. *Lancet*, 2, 1366-9.
- GATTINONI, L., SPEISER, D. E., LICHTERFELD, M. & BONINI, C. 2017. T memory stem cells in health and disease. *Nat Med*, 23, 18-27.
- HACEIN-BEY-ABINA, S., GARRIGUE, A., WANG, G. P., SOULIER, J., LIM, A., MORILLON, E., CLAPPIER, E., CACCAVELLI, L., DELABESSE, E., BELDJORD, K., ASNAFI, V., MACINTYRE, E., DAL CORTIVO, L.,

- RADFORD, I., BROUSSE, N., SIGAUX, F., MOSHOUS, D., HAUER, J., BORKHARDT, A., BELOHRADSKY, B. H., WINTERGERST, U., VELEZ, M. C., LEIVA, L., SORENSEN, R., WULFFRAAT, N., BLANCHE, S., BUSHMAN, F. D., FISCHER, A. & CAVAZZANA-CALVO, M. 2008. Insertional oncogenesis in 4 patients after retrovirus-mediated gene therapy of SCID-X1. *J Clin Invest*, 118, 3132-42.
- HACEIN-BEY-ABINA, S., VON KALLE, C., SCHMIDT, M., LE DEIST, F., WULFFRAAT, N., MCINTYRE, E., RADFORD, I., VILLEVAL, J. L., FRASER, C. C., CAVAZZANA-CALVO, M. & FISCHER, A. 2003. A serious adverse event after successful gene therapy for X-linked severe combined immunodeficiency. *N Engl J Med*, 348, 255-6.
- HADDAD, E. & HOENIG, M. 2019. Hematopoietic Stem Cell Transplantation for Severe Combined Immunodeficiency (SCID). *Front Pediatr*, 7, 481.
- HARTLERODE, A. J. & SCULLY, R. 2009. Mechanisms of double-strand break repair in somatic mammalian cells. *Biochem J*, 423, 157-68.
- HER, J. & BUNTING, S. F. 2018. How cells ensure correct repair of DNA double-strand breaks. *J Biol Chem*, 293, 10502-10511.
- HIRAMOTO, T., LI, L. B., FUNK, S. E., HIRATA, R. K. & RUSSELL, D. W. 2018. Nuclease-free Adeno-Associated Virus-Mediated IL2rg Gene Editing in X-SCID Mice. *Mol Ther*, 26, 1255-1265.
- HOLGATE, S. T. & POLOSA, R. 2008. Treatment strategies for allergy and asthma. *Nat Rev Immunol*, 8, 218-30.
- HOU, Y., GRATZ, H. P., UREÑA-BAILÉN, G., GRATZ, P. G., SCHILBACH-STÜCKLE, K., RENNO, T., GÜNGÖR, D., MADER, D. A., MALENKE, E., ANTONY, J. S., HANDGRETINGER, R. & MEZGER, M. 2021. Somatic Reversion of a Novel IL2RG Mutation Resulting in Atypical X-Linked Combined Immunodeficiency. *Genes (Basel)*, 13.
- HOU, Y., UREÑA-BAILÉN, G., MOHAMMADIAN GOL, T., GRATZ, P. G., GRATZ, H. P., ROIG-MERINO, A., ANTONY, J. S., LAMSFUS-CALLE, A., DANIEL-MORENO, A., HANDGRETINGER, R. & MEZGER, M. 2022. Challenges in Gene Therapy for Somatic Reverted Mosaicism in X-Linked Combined Immunodeficiency by CRISPR/Cas9 and Prime Editing. *Genes (Basel)*, 13.
- HSU, A. P., PITTALUGA, S., MARTINEZ, B., RUMP, A. P., RAFFELD, M., UZEL, G., PUCK, J. M., FREEMAN, A. F. & HOLLAND, S. M. 2015. IL2RG reversion event in a common lymphoid progenitor leads to delayed diagnosis and milder phenotype. *J Clin Immunol*, 35, 449-53.
- HSU, P. D., LANDER, E. S. & ZHANG, F. 2014. Development and applications of CRISPR-Cas9 for genome engineering. *Cell*, 157, 1262-1278.
- KAWAI, T., SAITO, M., NISHIKOMORI, R., YASUMI, T., IZAWA, K., MURAKAMI, T., OKAMOTO, S., MORI, Y., NAKAGAWA, N., IMAI, K., NONOYAMA, S., WADA, T., YACHIE, A., OHMORI, K., NAKAHATA, T. & HEIKE, T. 2012. Multiple reversions of an IL2RG mutation restore T cell function in an X-linked severe combined immunodeficiency patient. *J Clin Immunol*, 32, 690-7.
- KIM, H. P., IMBERT, J. & LEONARD, W. J. 2006. Both integrated and differential regulation of components of the IL-2/IL-2 receptor system. *Cytokine Growth Factor Rev*, 17, 349-66.

- KING, J. R. & HAMMARSTRÖM, L. 2018. Newborn Screening for Primary Immunodeficiency Diseases: History, Current and Future Practice. *J Clin Immunol*, 38, 56-66.
- KUIJPERS, T. W., VAN LEEUWEN, E. M., BARENDREGT, B. H., KLARENBECK, P., AAN DE KERK, D. J., BAARS, P. A., JANSEN, M. H., DE VRIES, N., VAN LIER, R. A. & VAN DER BURG, M. 2013. A reversion of an IL2RG mutation in combined immunodeficiency providing competitive advantage to the majority of CD8+ T cells. *Haematologica*, 98, 1030-8.
- KURY, P., FÜHRER, M., FUCHS, S., LORENZ, M. R., GIORGETTI, O. B., BAKHTIAR, S., FREI, A. P., FISCH, P., BOEHM, T., SCHWARZ, K., SPECKMANN, C. & EHL, S. 2020. Long-term robustness of a T-cell system emerging from somatic rescue of a genetic block in T-cell development. *EBioMedicine*, 59, 102961.
- LAMSFUS-CALLE, A., DANIEL-MORENO, A., UREÑA-BAILÉN, G., ROTTENBERGER, J., RAJU, J., EPTING, T., MARCIANO, S., HEUMOS, L., BASKARAN, P., J, S. A., HANDGRETINGER, R. & MEZGER, M. 2021. Universal Gene Correction Approaches for  $\beta$ -hemoglobinopathies Using CRISPR-Cas9 and Adeno-Associated Virus Serotype 6 Donor Templates. *Crispr j*, 4, 207-222.
- LANKESTER, A. C., ALBERT, M. H., BOOTH, C., GENNERY, A. R., GÜNGÖR, T., HÖNIG, M., MORRIS, E. C., MOSHOUS, D., NEVEN, B., SCHULZ, A., SLATTER, M. & VEYS, P. 2021. EBMT/ESID inborn errors working party guidelines for hematopoietic stem cell transplantation for inborn errors of immunity. *Bone Marrow Transplant*, 56, 2052-2062.
- LEONARD, W. J. & SPOLSKI, R. 2005. Interleukin-21: a modulator of lymphoid proliferation, apoptosis and differentiation. *Nat Rev Immunol*, 5, 688-98.
- LI, H., BUSQUETS, O., VERMA, Y., SYED, K. M., KUTNOWSKI, N., PANGILINAN, G. R., GILBERT, L. A., BATEUP, H. S., RIO, D. C., HOCKEMEYER, D. & SOLDNER, F. 2022. Highly efficient generation of isogenic pluripotent stem cell models using prime editing. *Elife*, 11.
- LIM, C. K., ABOLHASSANI, H., APPELBERG, S. K., SUNDIN, M. & HAMMARSTRÖM, L. 2019. IL2RG hypomorphic mutation: identification of a novel pathogenic mutation in exon 8 and a review of the literature. *Allergy Asthma Clin Immunol*, 15, 2.
- LIN, C. H., KUEHN, H. S., THAULAND, T. J., LEE, C. M., DE RAVIN, S. S., MALECH, H. L., KEYES, T. J., JAGER, A., DAVIS, K. L., GARCIA-LLORET, M. I., ROSENZWEIG, S. D. & BUTTE, M. J. 2020. Progressive B Cell Loss in Revertant X-SCID. *J Clin Immunol*, 40, 1001-1009.
- LIU, M., REHMAN, S., TANG, X., GU, K., FAN, Q., CHEN, D. & MA, W. 2018. Methodologies for Improving HDR Efficiency. *Front Genet*, 9, 691.
- MAMCARZ, E., ZHOU, S., LOCKEY, T., ABDELSAMED, H., CROSS, S. J., KANG, G., MA, Z., CONDORI, J., DOWDY, J., TRIPLETT, B., LI, C., MARON, G., ALDAVE BECERRA, J. C., CHURCH, J. A., DOKMECI, E., LOVE, J. T., DA MATTA AIN, A. C., VAN DER WATT, H., TANG, X., JANSSEN, W., RYU, B. Y., DE RAVIN, S. S., WEISS, M. J., YOUNGBLOOD, B., LONG-BOYLE, J. R., GOTTSCHALK, S., MEAGHER, M. M., MALECH, H. L., PUCK, J. M., COWAN, M. J. & SORRENTINO, B. P.

2019. Lentiviral Gene Therapy Combined with Low-Dose Busulfan in Infants with SCID-X1. *N Engl J Med*, 380, 1525-1534.
- MEDLEY, J. C., HEBBAR, S., SYDZYIK, J. T. & ZINOVYEVA, A. Y. 2022. Single nucleotide substitutions effectively block Cas9 and allow for scarless genome editing in *Caenorhabditis elegans*. *Genetics*, 220.
- MELLA, P., IMBERTI, L., BRUGNONI, D., PIROVANO, S., CANDOTTI, F., MAZZOLARI, E., BETTINARDI, A., FIORINI, M., DE MATTIA, D., MARTIRE, B., PLEBANI, A., NOTARANGELO, L. D. & GILIANI, S. 2000. Development of autologous T lymphocytes in two males with X-linked severe combined immune deficiency: molecular and cellular characterization. *Clin Immunol*, 95, 39-50.
- MENON, T., FIRTH, A. L., SCRIPTURE-ADAMS, D. D., GALIC, Z., QUALLS, S. J., GILMORE, W. B., KE, E., SINGER, O., ANDERSON, L. S., BORNZIN, A. R., ALEXANDER, I. E., ZACK, J. A. & VERMA, I. M. 2015. Lymphoid regeneration from gene-corrected SCID-X1 subject-derived iPSCs. *Cell Stem Cell*, 16, 367-72.
- MIYAZAWA, H. & WADA, T. 2021. Reversion Mosaicism in Primary Immunodeficiency Diseases. *Front Immunol*, 12, 783022.
- NOGUCHI, M., YI, H., ROSENBLATT, H. M., FILIPOVICH, A. H., ADELSTEIN, S., MODI, W. S., MCBRIDE, O. W. & LEONARD, W. J. 1993. Interleukin-2 receptor gamma chain mutation results in X-linked severe combined immunodeficiency in humans. *Cell*, 73, 147-57.
- OKAMOTO, S., AMAISHI, Y., MAKI, I., ENOKI, T. & MINENO, J. 2019. Highly efficient genome editing for single-base substitutions using optimized ssODNs with Cas9-RNPs. *Sci Rep*, 9, 4811.
- OKUNO, Y., HOSHINO, A., MURAMATSU, H., KAWASHIMA, N., WANG, X., YOSHIDA, K., WADA, T., GUNJI, M., TOMA, T., KATO, T., SHIRAISHI, Y., IWATA, A., HORI, T., KITO, T., CHIBA, K., TANAKA, H., SANADA, M., TAKAHASHI, Y., NONOYAMA, S., ITO, M., MIYANO, S., OGAWA, S., KOJIMA, S. & KANEGANE, H. 2015. Late-Onset Combined Immunodeficiency with a Novel IL2RG Mutation and Probable Revertant Somatic Mosaicism. *J Clin Immunol*, 35, 610-4.
- OSBORN, M. J., WEBBER, B. R., KNIPPING, F., LONETREE, C. L., TENNIS, N., DEFEO, A. P., MCELROY, A. N., STARKER, C. G., LEE, C., MERKEL, S., LUND, T. C., KELLY-SPRATT, K. S., JENSEN, M. C., VOYTAS, D. F., VON KALLE, C., SCHMIDT, M., GABRIEL, R., HIPPEN, K. L., MILLER, J. S., SCHARENBERG, A. M., TOLAR, J. & BLAZAR, B. R. 2016. Evaluation of TCR Gene Editing Achieved by TALENs, CRISPR/Cas9, and megaTAL Nucleases. *Mol Ther*, 24, 570-81.
- PALENDIRA, U., LOW, C., BELL, A. I., MA, C. S., ABBOTT, R. J., PHAN, T. G., RIMINTON, D. S., CHOO, S., SMART, J. M., LOUGARIS, V., GILIANI, S., BUCKLEY, R. H., GRIMBACHER, B., ALVARO, F., KLION, A. D., NICHOLS, K. E., ADELSTEIN, S., RICKINSON, A. B. & TANGYE, S. G. 2012. Expansion of somatically reverted memory CD8+ T cells in patients with X-linked lymphoproliferative disease caused by selective pressure from Epstein-Barr virus. *J Exp Med*, 209, 913-24.
- PAQUET, D., KWART, D., CHEN, A., SPROUL, A., JACOB, S., TEO, S., OLSEN, K. M., GREGG, A., NOGGLE, S. & TESSIER-LAVIGNE, M. 2016.

- Efficient introduction of specific homozygous and heterozygous mutations using CRISPR/Cas9. *Nature*, 533, 125-9.
- PARRISH, Y. K., BAEZ, I., MILFORD, T. A., BENITEZ, A., GALLOWAY, N., ROGERIO, J. W., SAHAKIAN, E., KAGODA, M., HUANG, G., HAO, Q. L., SEVILLA, Y., BARSKY, L. W., ZIELINSKA, E., PRICE, M. A., WALL, N. R., DOVAT, S. & PAYNE, K. J. 2009. IL-7 Dependence in human B lymphopoiesis increases during progression of ontogeny from cord blood to bone marrow. *J Immunol*, 182, 4255-66.
- PAVEL-DINU, M., WIEBKING, V., DEJENE, B. T., SRIFA, W., MANTRI, S., NICOLAS, C. E., LEE, C., BAO, G., KILDEBECK, E. J., PUNJYA, N., SINDHU, C., INLAY, M. A., SAXENA, N., DERAVIN, S. S., MALECH, H., RONCAROLO, M. G., WEINBERG, K. I. & PORTEUS, M. H. 2019. Gene correction for SCID-X1 in long-term hematopoietic stem cells. *Nat Commun*, 10, 1634.
- PROFAIZER, T. & SLEV, P. 2020. A Multiplex, Droplet Digital PCR Assay for the Detection of T-Cell Receptor Excision Circles and Kappa-Deleting Recombination Excision Circles. *Clin Chem*, 66, 229-238.
- PUCK, J. M., DESCHÊNES, S. M., PORTER, J. C., DUTRA, A. S., BROWN, C. J., WILLARD, H. F. & HENTHORN, P. S. 1993. The interleukin-2 receptor gamma chain maps to Xq13.1 and is mutated in X-linked severe combined immunodeficiency, SCIDX1. *Hum Mol Genet*, 2, 1099-104.
- REVY, P., KANNENGIESSER, C. & FISCHER, A. 2019. Somatic genetic rescue in Mendelian haematopoietic diseases. *Nat Rev Genet*, 20, 582-598.
- ROCHMAN, Y., SPOLSKI, R. & LEONARD, W. J. 2009. New insights into the regulation of T cells by gamma(c) family cytokines. *Nat Rev Immunol*, 9, 480-90.
- ROMERO, Z., LOMOVA, A., SAID, S., MIGGELBRINK, A., KUO, C. Y., CAMPO-FERNANDEZ, B., HOBAN, M. D., MASIUK, K. E., CLARK, D. N., LONG, J., SANCHEZ, J. M., VELEZ, M., MIYAHIRA, E., ZHANG, R., BROWN, D., WANG, X., KURMANGALIYEV, Y. Z., HOLLIS, R. P. & KOHN, D. B. 2019. Editing the Sickle Cell Disease Mutation in Human Hematopoietic Stem Cells: Comparison of Endonucleases and Homologous Donor Templates. *Mol Ther*, 27, 1389-1406.
- SAKAGUCHI, S., YAMAGUCHI, T., NOMURA, T. & ONO, M. 2008. Regulatory T cells and immune tolerance. *Cell*, 133, 775-87.
- SCHIROLI, G., FERRARI, S., CONWAY, A., JACOB, A., CAPO, V., ALBANO, L., PLATI, T., CASTIELLO, M. C., SANVITO, F., GENNERY, A. R., BOVOLENTA, C., PALCHAUDHURI, R., SCADDEN, D. T., HOLMES, M. C., VILLA, A., SITIA, G., LOMBARDO, A., GENOVESE, P. & NALDINI, L. 2017. Preclinical modeling highlights the therapeutic potential of hematopoietic stem cell gene editing for correction of SCID-X1. *Sci Transl Med*, 9.
- SPECKMANN, C., PANNICKE, U., WIECH, E., SCHWARZ, K., FISCH, P., FRIEDRICH, W., NIEHUES, T., GILMOUR, K., BUITING, K., SCHLESIER, M., EIBEL, H., ROHR, J., SUPERTI-FURGA, A., GROSS-WIELTSCH, U. & EHL, S. 2008. Clinical and immunologic consequences of a somatic reversion in a patient with X-linked severe combined immunodeficiency. *Blood*, 112, 4090-7.

- SPOLSKI, R. & LEONARD, W. J. 2008. Interleukin-21: basic biology and implications for cancer and autoimmunity. *Annu Rev Immunol*, 26, 57-79.
- STEPHAN, V., WAHN, V., LE DEIST, F., DIRKSEN, U., BROKER, B., MÜLLER-FLECKENSTEIN, I., HORNEFF, G., SCHROTEN, H., FISCHER, A. & DE SAINT BASILE, G. 1996. Atypical X-linked severe combined immunodeficiency due to possible spontaneous reversion of the genetic defect in T cells. *N Engl J Med*, 335, 1563-7.
- SURH, C. D. & SPRENT, J. 2008. Homeostasis of naive and memory T cells. *Immunity*, 29, 848-62.
- SYMINGTON, L. S. & GAUTIER, J. 2011. Double-strand break end resection and repair pathway choice. *Annu Rev Genet*, 45, 247-71.
- TSIATIS, A. C., NORRIS-KIRBY, A., RICH, R. G., HAFEZ, M. J., GOCKE, C. D., ESHLEMAN, J. R. & MURPHY, K. M. 2010. Comparison of Sanger sequencing, pyrosequencing, and melting curve analysis for the detection of KRAS mutations: diagnostic and clinical implications. *J Mol Diagn*, 12, 425-32.
- VELDHOEN, M., UYTENHOVE, C., VAN SNICK, J., HELMBY, H., WESTENDORF, A., BUER, J., MARTIN, B., WILHELM, C. & STOCKINGER, B. 2008. Transforming growth factor-beta 'reprograms' the differentiation of T helper 2 cells and promotes an interleukin 9-producing subset. *Nat Immunol*, 9, 1341-6.
- WANG, X., LUPARDUS, P., LAPORTE, S. L. & GARCIA, K. C. 2009. Structural biology of shared cytokine receptors. *Annu Rev Immunol*, 27, 29-60.
- WANG, X., RICKERT, M. & GARCIA, K. C. 2005. Structure of the quaternary complex of interleukin-2 with its alpha, beta, and gamma receptors. *Science*, 310, 1159-63.
- WEN, J., TAO, W., HAO, S. & ZU, Y. 2017. Cellular function reinstatement of offspring red blood cells cloned from the sickle cell disease patient blood post CRISPR genome editing. *J Hematol Oncol*, 10, 119.

## 7. Declaration of Contributions to the Dissertation

All work presented in the dissertation was carried out in the Department of General Paediatrics, Haematology/Oncology, Children's Hospital of Tübingen University.

The dissertation was completed under the supervision of Dr.Dr. Markus Mezger and Prof. Dr. Rupert Handgretinger. The subjects of patients were coordinated by Prof. Dr. Rupert Handgretinger. Dr.Dr. Markus Mezger, Dr. Justin Antony Selvaraj, Dr. Tahereh Mohammadian Gol, Guillermo Ureña-Bailén and I designed the experiments. The transfection protocol establishment of CRISPR/Cas9 and prime editing were assisted by Dr. Alicia Roig-Merino. After training, all experiments were carried out by myself. The results and conclusions were analyzed by myself and discussed with Dr.Dr. Markus Mezger, Dr. Tahereh Mohammadian Gol and Guillermo Ureña-Bailén. With the consent of the co-authors and the permission of the journal, some of my results in the related publication are incorporated into this thesis with appropriate citations.

I hereby declare that this dissertation is done by myself, all the presented data was from my own research work, and any additional sources of information have been suitably cited.

I confirm that this dissertation has not been submitted for any other degree or professional qualification.

Tuebingen, 28.11.2022, Yujuan Hou

---

Place/date/signature of doctoral candidate

## 8. Publications

1. **Hou Y\***, Gratz HP\*, Ureña-Bailén G, Gratz PG, Schilbach-Stückle K, Renno T, Güngör D, Mader DA, Malenke E, Antony JS, Handgretinger R, Mezger M. Somatic Reversion of a Novel *IL2RG* Mutation Resulting in Atypical X-Linked Combined Immunodeficiency. *Genes*. 2021.

2. **Hou Y\***, Ureña-Bailén G, Gol MT, Gratz PG, Gratz HP, Roig-Merino A, Antony JS, Lamsfus-Calle A, Daniel-Moreno A, Handgretinger R and Mezger M. Challenge in Gene Therapy for Somatic Reverted Mosaicism of X-linked Combined Immunodeficiency by CRISPR/Cas9 and Prime Editing. *Genes*. 2022.

## 9. Acknowledgments

My sincere appreciation first goes to Dr. Dr. Markus Mezger, my primary supervisor. He is erudite, responsible, and motivated for research and clinical work. Thanks to him, I could have the opportunity to come to the Children's Hospital and Medical Faculty of the university of Tübingen. His encouragement and guidance made me grow significantly in the research field and accomplish my dissertation. I also would like to express my gratitude to Prof. Dr. med. Rupert Handgretinger for his supervision and great support on my project. I am grateful to Dr. Justin Antony Selvaraj for his informative comments on my research and publications. I do appreciate Dr. Tahereh Mohammadian Gol, who has supported and guided me in many important experiments. She kindly cheered me up when I was feeling frustrated. I really appreciate her constructive comments improving this thesis.

I would like to thank the research team of AG Mezger (Guillermo Ureña Bailén, Hans Peter Gratz, Paul Gratz, Luise Luib, Dr. Alberto Daniel Moreno, Dr. Andrés Lamsfus-Calle, Ralph Sinn) and other colleagues (Janani Raju, Derya Güngör, Vidiyaah Santhanakumaran) for their unconditionally support all the time. I would never forget this precious time we spent together. Special thanks to Guillermo, my lab counselor/buddy, who has saved my life in every challenging moment in the lab. I have gotten so much helpful experience and advice from him. He has inspired me to complete this project successfully.

I am much obliged to my parents for their support and understanding in my life, study and work. Last but foremost, a thousand thanks to my soulmate, Hao Wang. Being far apart from distant oceans, we have suffered from missing each other for three years. His encouragement, guardianship, and sacrifices enabled me to complete my doctoral degree with determination.

I will always remember the wonderful period in the beautiful and historic university town of Tübingen.